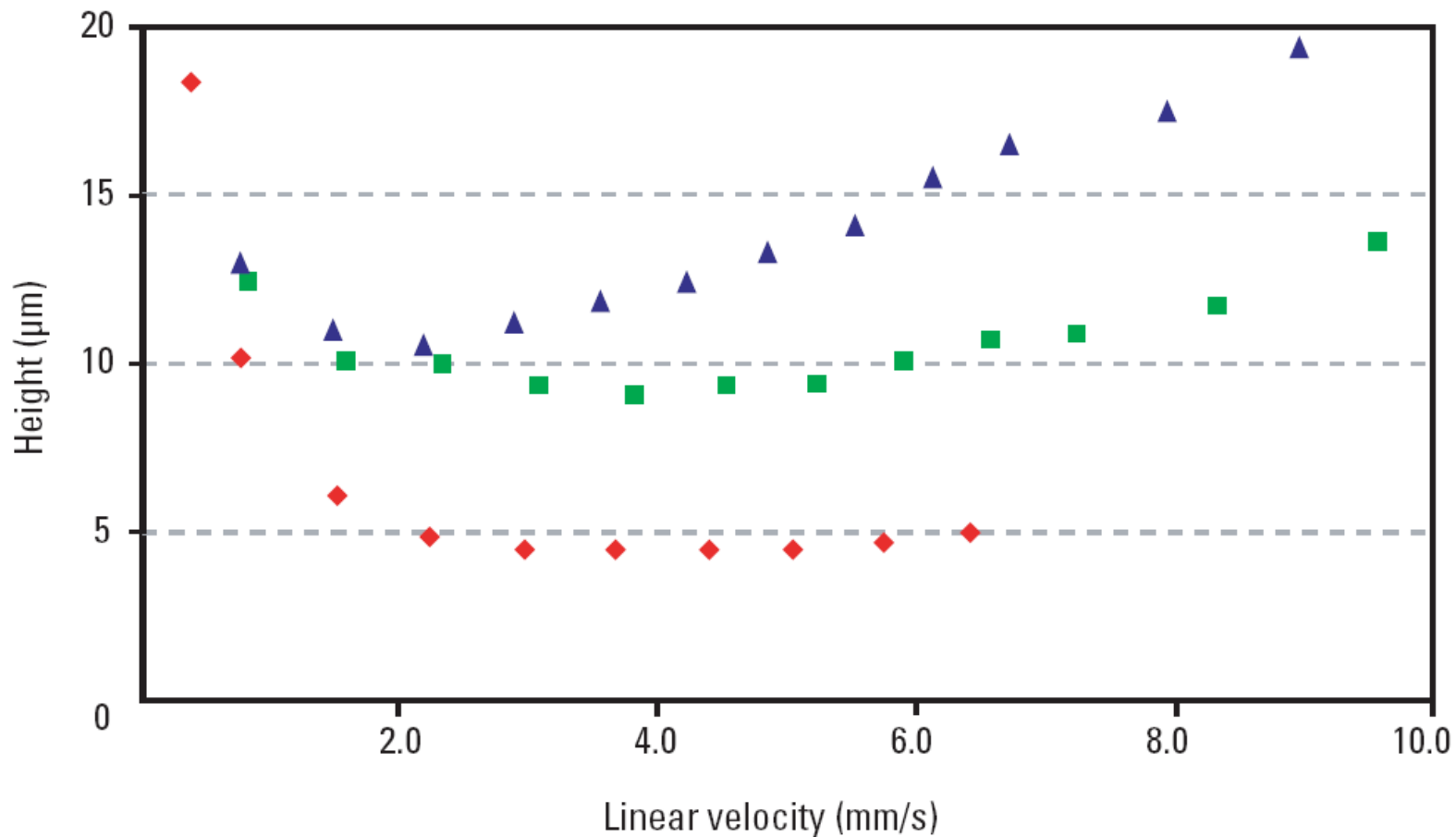


# Ultra and nano High Performance Liquid Chromatography

# Why miniaturization?

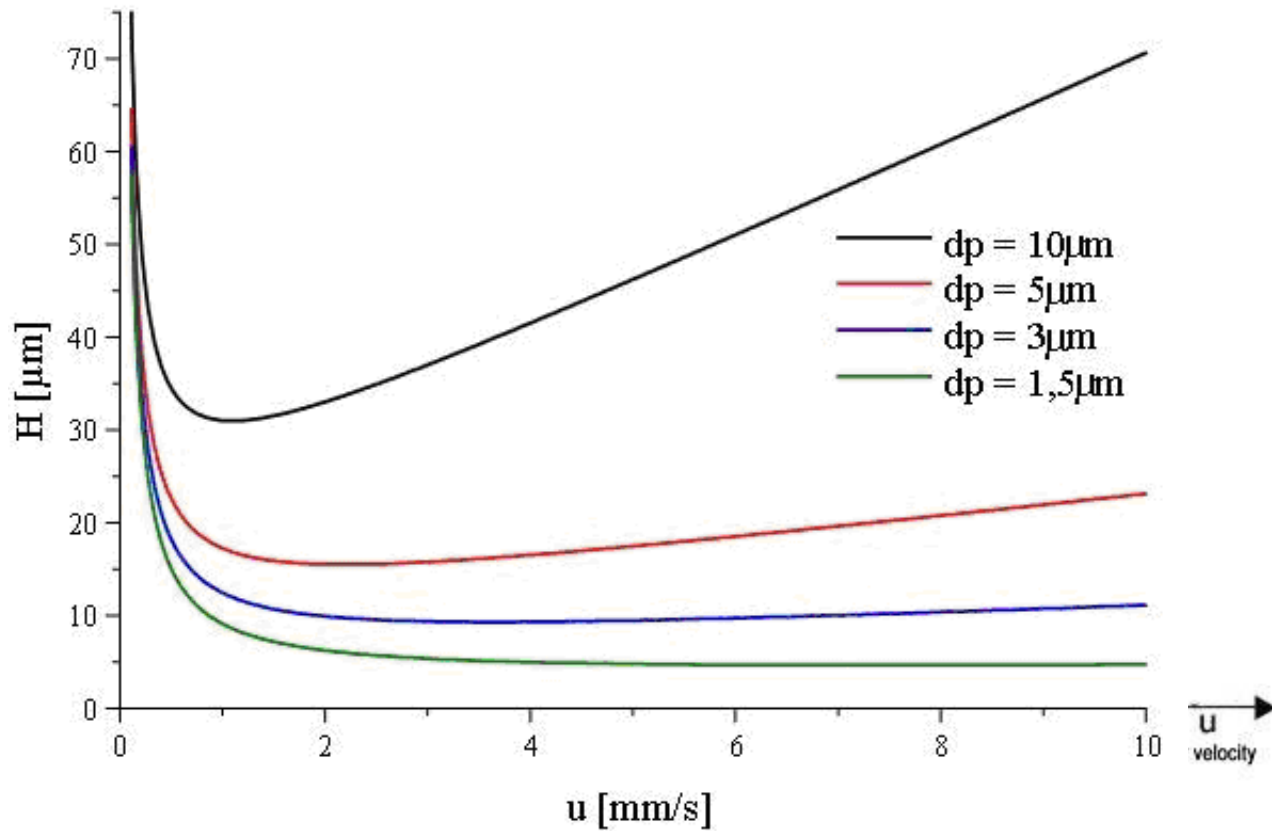
- i) increased mass sensitivity owing to the reduced chromatographic dilution,
- ii) the use of smaller particle sizes ( $<3 \mu\text{m}$ ),
- iii) lower stationary phase, solvent, and sample volume consumption,
- iv) the compatibility with flow rate requirements of a nanospray interface for on-line coupling to mass spectrometry (MS).



Van Deemter curves for hexylbenzene on particles that are 1.7  $\mu\text{m}$  (red diamonds), 3.5  $\mu\text{m}$  (green squares), and 5.0  $\mu\text{m}$  (blue triangles) in diameter.

# Why Ultra High Performance LC (UHPLC)?

$$H = A + \frac{B}{u} + C * u$$



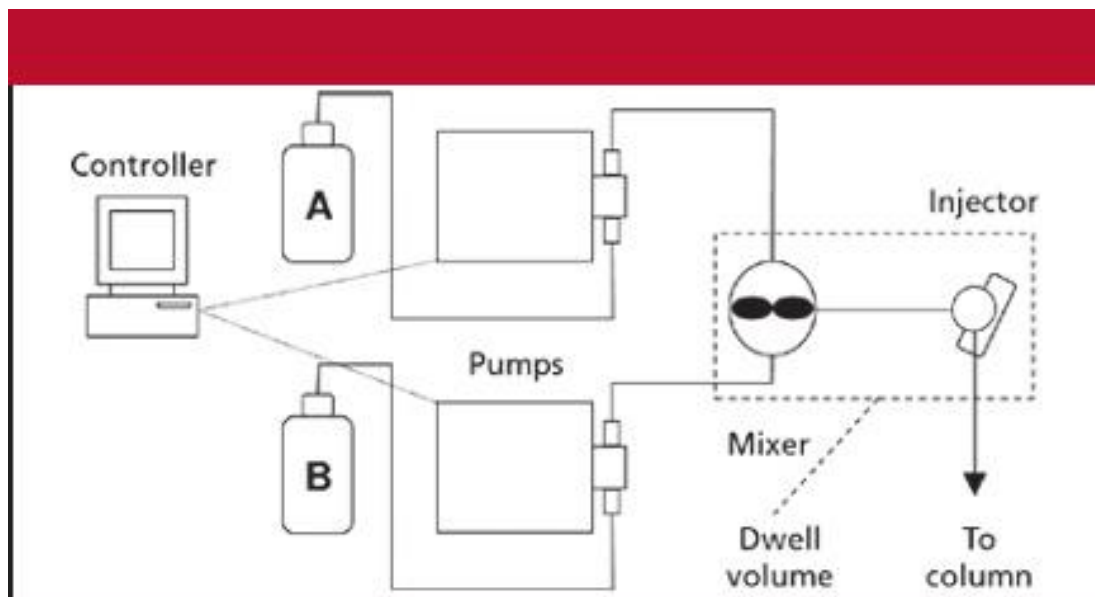
# UPLC Conditions

If instruments with extended pressure range were available and smaller particles could be used, then a higher separation performance or a faster analysis could be achieved, compared with classical HPLC. The term ultra-high-pressure LC was introduced to define the use of sub-2- $\mu\text{m}$  particles packed into very long (>150-mm) capillary columns (<50- $\mu\text{m}$  i.d.) that ran at pressures up to 700 MPa.

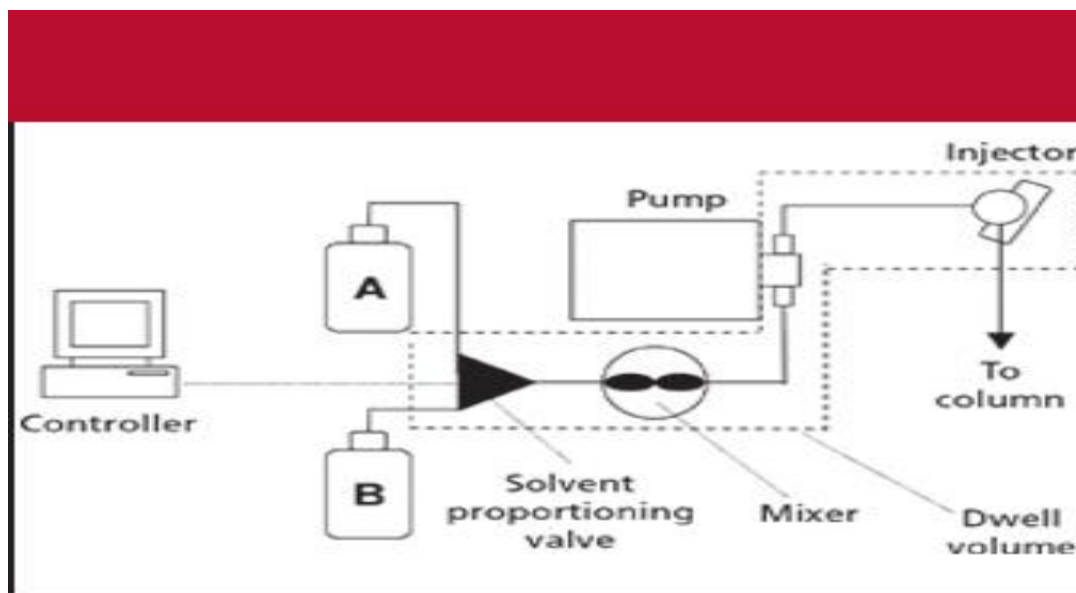
# Dwell volume

- The dwell volume is the system volume from the point at which the mobile phase solvents are mixed until they reach the head of the column.

Dwell volume in High Pressure: Mixer, connecting Tubing and autosampler loop (1-3 mL)



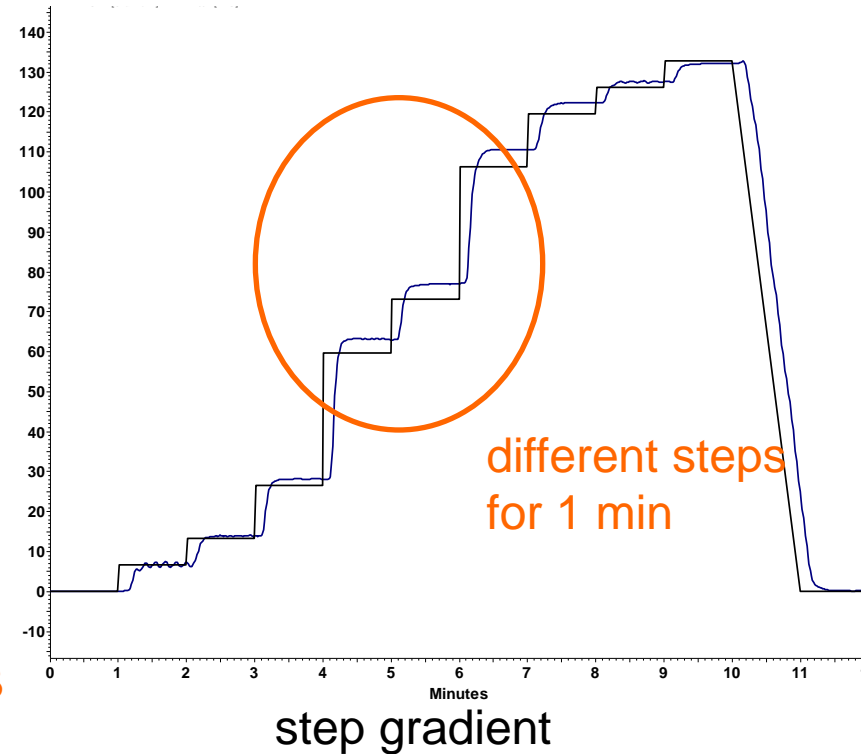
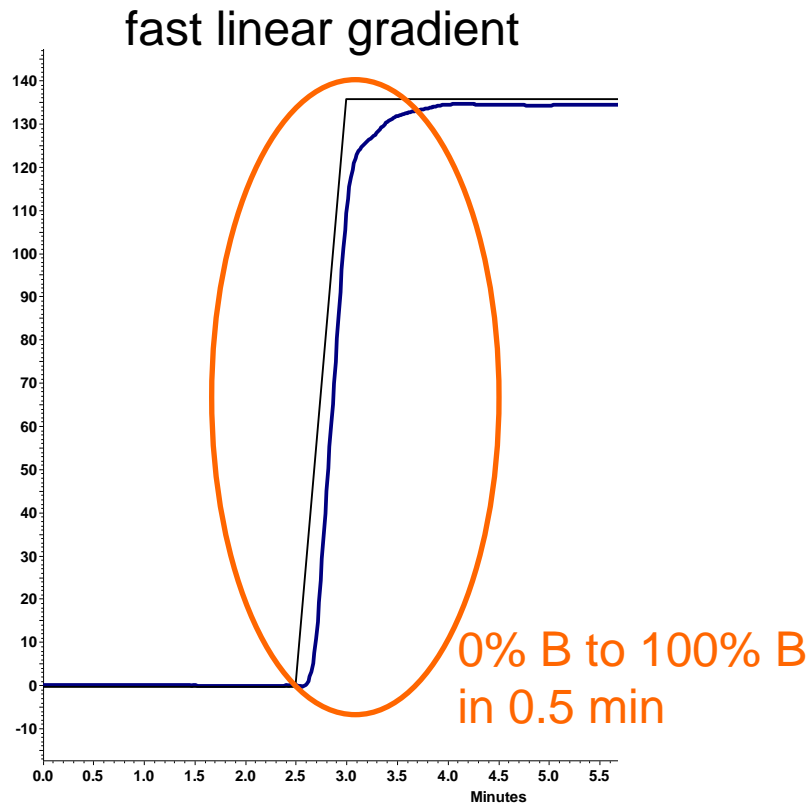
Dwell volume in Low Pressure: Mixer, connecting Tubing, autosampler loop, additional tubing and pump head (2-4 mL)



# UHPLC

- System Adaption: gradient test / dwell volume

dwell volume:  $< 115 \mu\text{l}$





# Dilution parameter

- The chromatographic dilution  $D$  at the end of the column is given by:

$$D = \frac{C_0}{C_{\max}} = \frac{E_t \pi r^2 (1 + K) \sqrt{2\pi LH}}{V_{inj}}$$

- $C_0$  is the initial compound concentration in a sample,
- $C_{\max}$  is the final compound concentration at max the peak maximum,
- $r$  is the column radius,
- $k$  is the retention factor,
- $L$  is the column length,
- $H$  is the column plate height,
- $E_t$  is the column porosity and
- $V_{inj}$  is the injected sample volume.
- $D$  increases proportionally with the square of the column radius and also with the square root of the column length and plate height of the column.

Hence, under identical chromatographic and injection conditions  $C_{\max}$  increases inversely to  $r^2$ . From this equation a 21.16-fold increase in peak height and mass sensitivity for a reduction in the diameter of a column from 4.6 mm to 1 mm I.D. can be calculated.

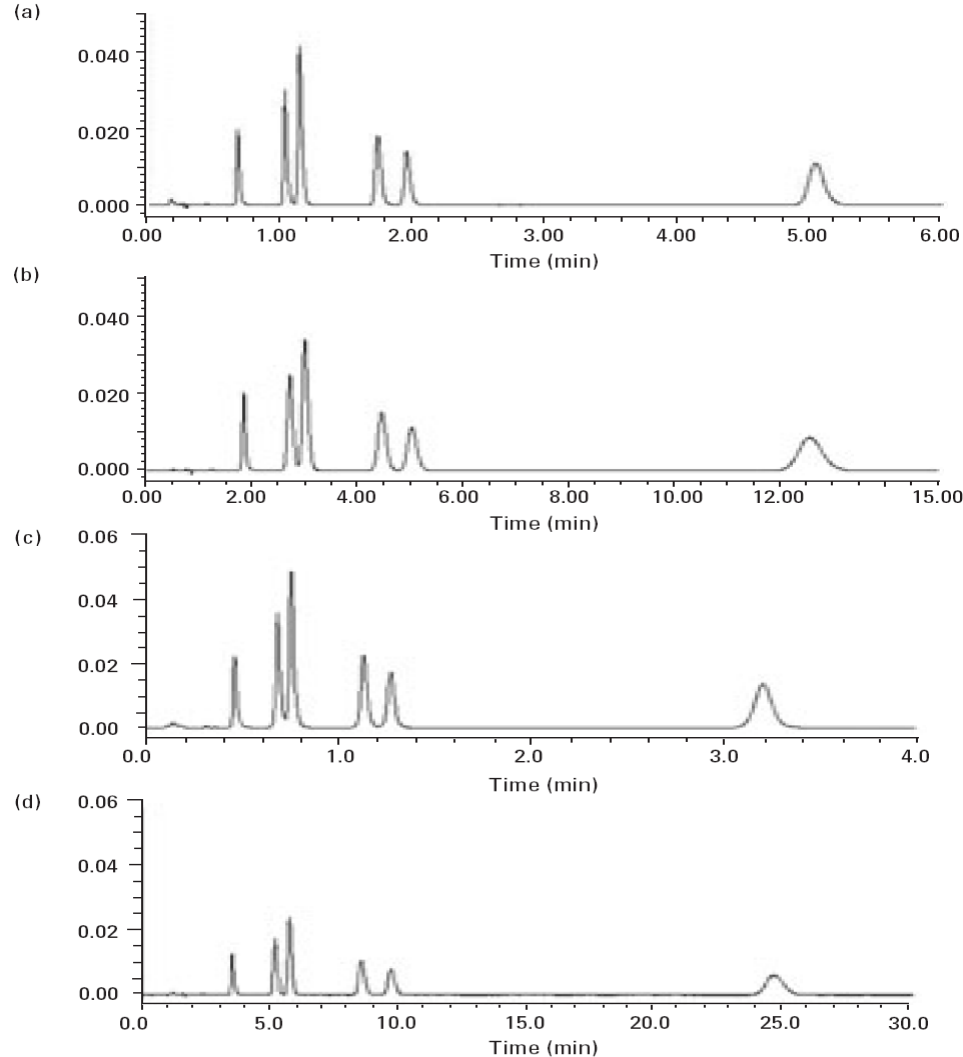
# Resolution

In isocratic separations, the resolution is proportional to the square root of efficiency. Particle size and efficiency at the optimum linear velocity are inversely proportional. Therefore, resolution is inversely proportional to the square root of particle size. With this knowledge, we can calculate that 1.7- $\mu\text{m}$  particles will offer 1.7 and 1.4 greater resolution than 5.0- $\mu\text{m}$  and 3.5- $\mu\text{m}$  particles, respectively, at equal column lengths.

# Analysis time

It is well established that column efficiency at the optimum linear velocity is proportional to column length  $L$  *divided by particle size*  $dp$ .

For example, with 1.7- $\mu\text{m}$  particles, column lengths that are 3 shorter than those used for 5.0- $\mu\text{m}$  particles will give the same efficiency and resolution. Because the optimum flow rate is 3 higher, the result is that the same resolution obtained with 5.0- $\mu\text{m}$  HPLC separations can be achieved 9 faster with 1.7- $\mu\text{m}$  particles in UPLC. In comparison with 3.5- $\mu\text{m}$  particles, the benefit with 1.7- $\mu\text{m}$  particles is a 4 shorter run time.



Separation on 50-mm columns packed with (a) 1.7- $\mu\text{m}$  and (b) 4.8- $\mu\text{m}$  particles; (c) 30-mm column packed with 1.7- $\mu\text{m}$  particles; (d) 100-mm column packed with 4.8- $\mu\text{m}$  particles. All columns are C18-bonded bridged-ethyl hybrid particles with 2.1-mm i.d. Pressures across columns are (a) 53, (b) 2.4, (c) 32, and (d) 4.8 MPa.

# Expected pressure

- Where  $\Delta p$  is the pressure drop across the column,  $F$  is the flow rate,  $\eta$  is the viscosity,  $L$  is the column length and  $r$  is the radius of the column ( $2r = d_c$ ). This prepared microcolumn has a lower diameter than conventional column (at least 4 times) and also,  $dp$  in this column is lower than conventional columns (3 versus 12  $\mu\text{m}$ ).
- Therefore, the 3-fold reduction in  $dp$  in UPLC translates to back pressures that are 27 higher compared with HPLC separations when 5- $\mu\text{m}$  particles are used.

$$\Delta p = \frac{F \eta L}{\pi r^2 d_p^2}$$

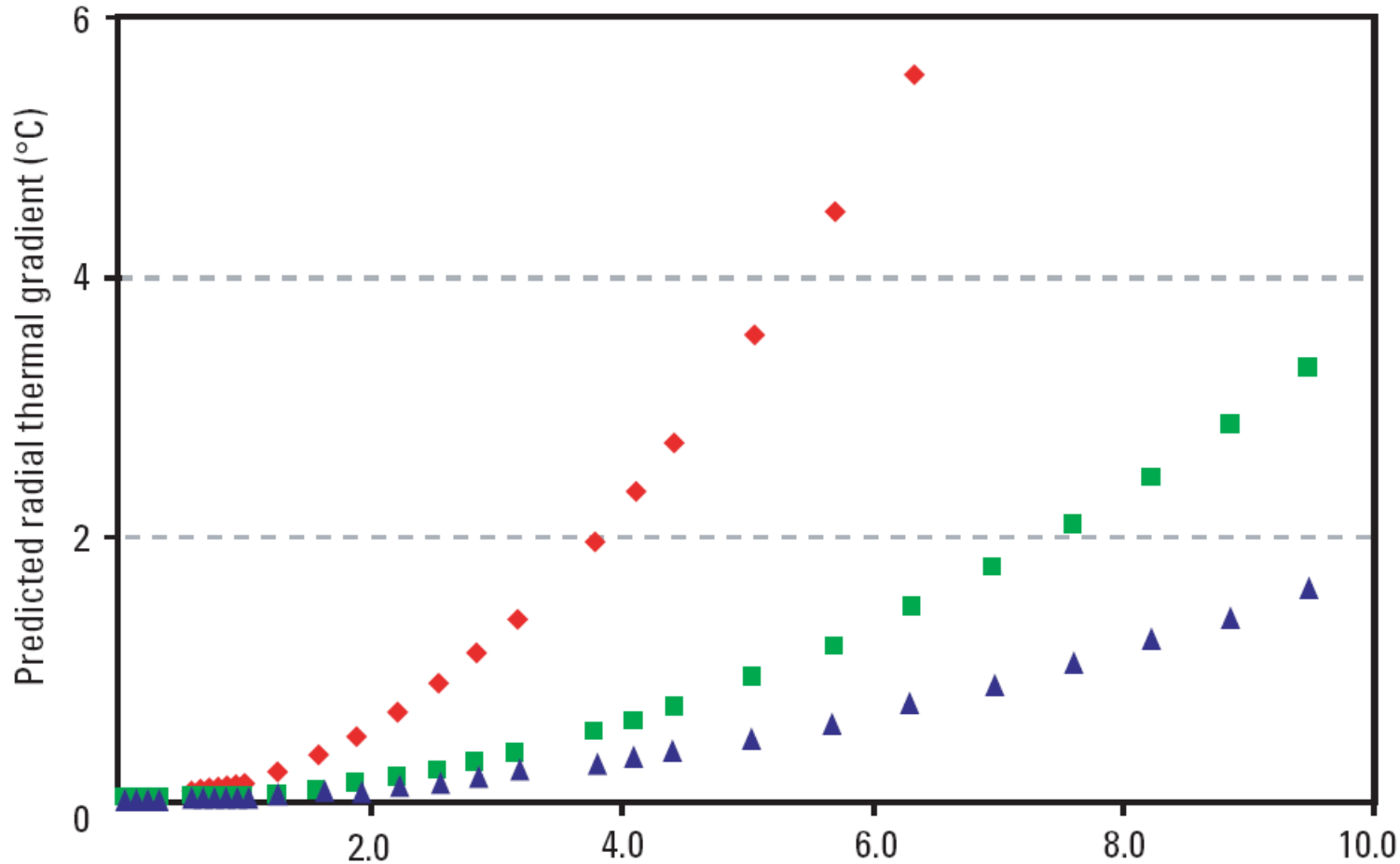
# Instrumentations

It follows that the instrumentation must be capable of operating at higher pressures. This includes fittings, pump seals, injector valves, and the chromatographic column.

The first commercial instrument designed for UPLC operation is rated for use up to 100 MPa. *This pressure limit* allows for the use of columns up to 150-mm long for small-molecule separations. The gradient system uses a four-piston pump in which the first two pistons pre-pressurize the solvents to be delivered by the high-pressure pistons.

# Temperature

- The maximum radial thermal gradient that develops along the *y axis is proportional to the superficial velocity of the mobile phase*, the pressure drop per unit length, and the square of the column radius. It is inversely proportional to the average effective heat conductivity of the column in the radial direction.



Radial thermal gradient vs linear velocity for hexylbenzene on particles that are 1.7 μm (red diamonds), 3.5 μm (green squares), and 5.0 μm (blue triangles) in diameter.

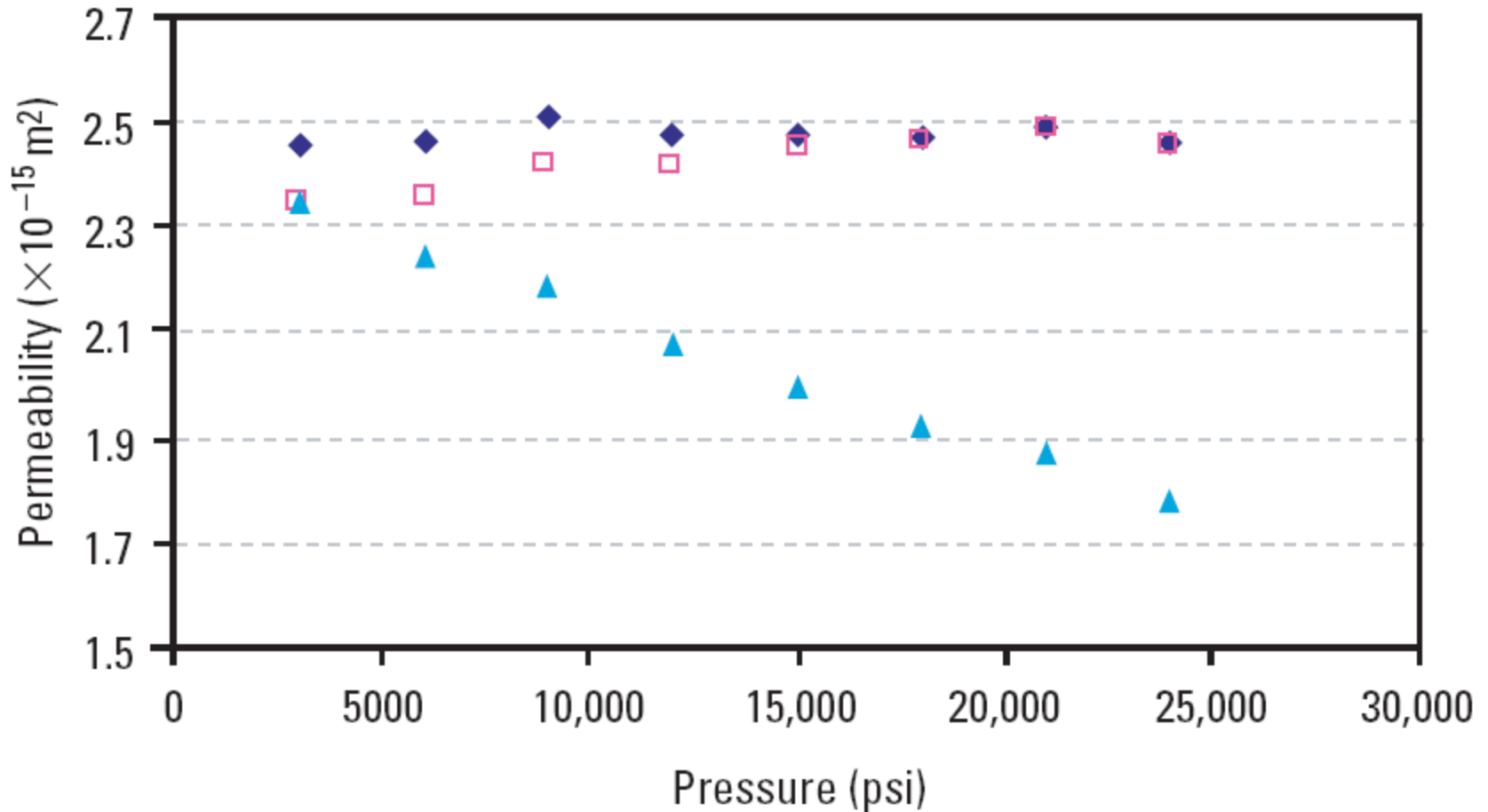


# Permeability

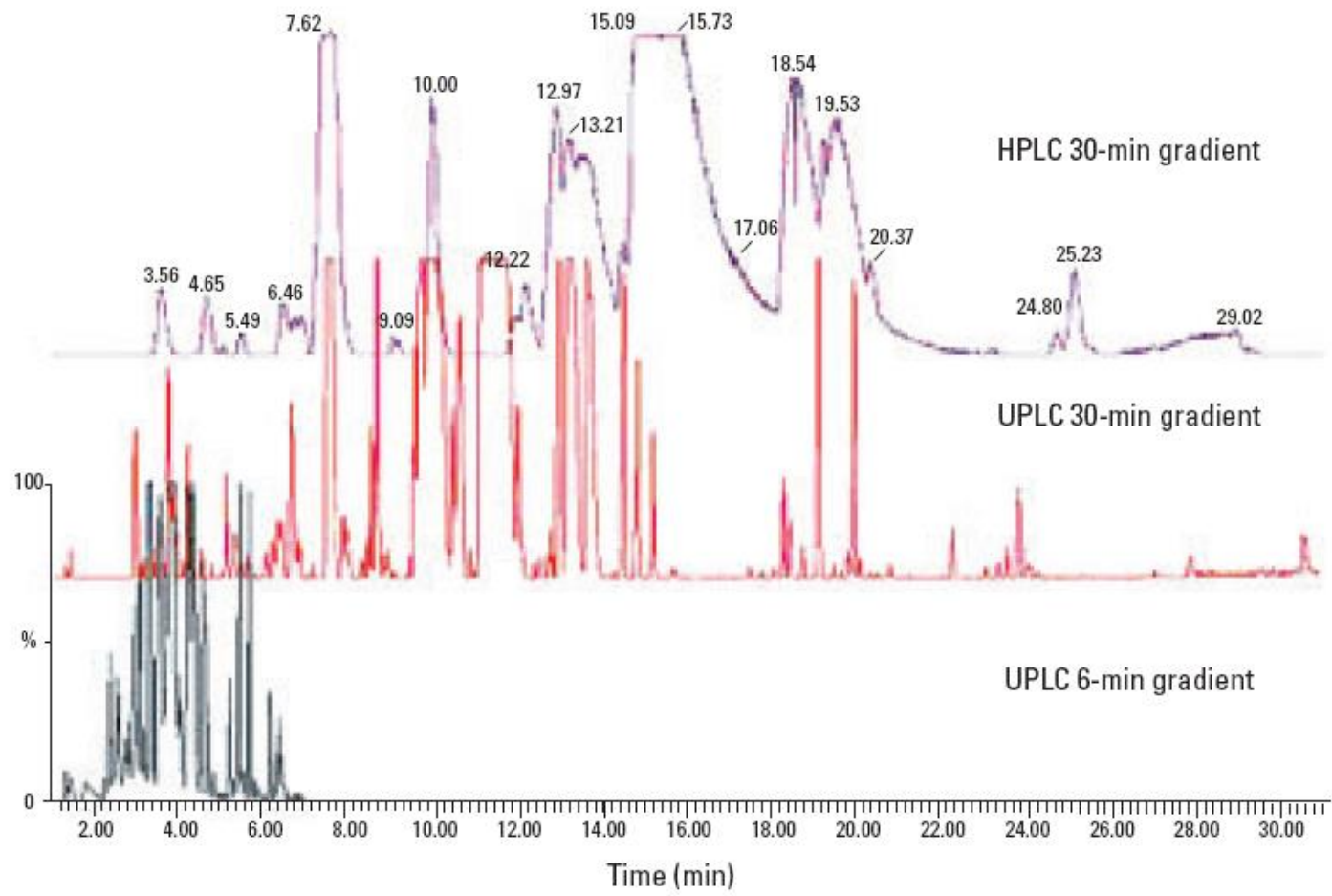
In the pioneering UPLC studies, monodisperse, nonporous particles were used. *Failed packing attempts* (3 lower efficiency) were also reported with porous particles of a wider *dp distribution*.

*Scanning electron micrographs* of packed capillary columns demonstrated a very tight and ordered bed structure with the uniformly sized nonporous particles. However, columns with porous packing material with a wide size distribution showed extensive nonuniformity.

The specific permeability  $K_0$  was calculated by using  $K_0 = FL/r^2P$ , in which  $F$  is the flow rate ( $m^3/s$ ),  $\eta$  is the solvent viscosity (cP), and  $P$  is the pressure drop ( $N/m^2$ ).

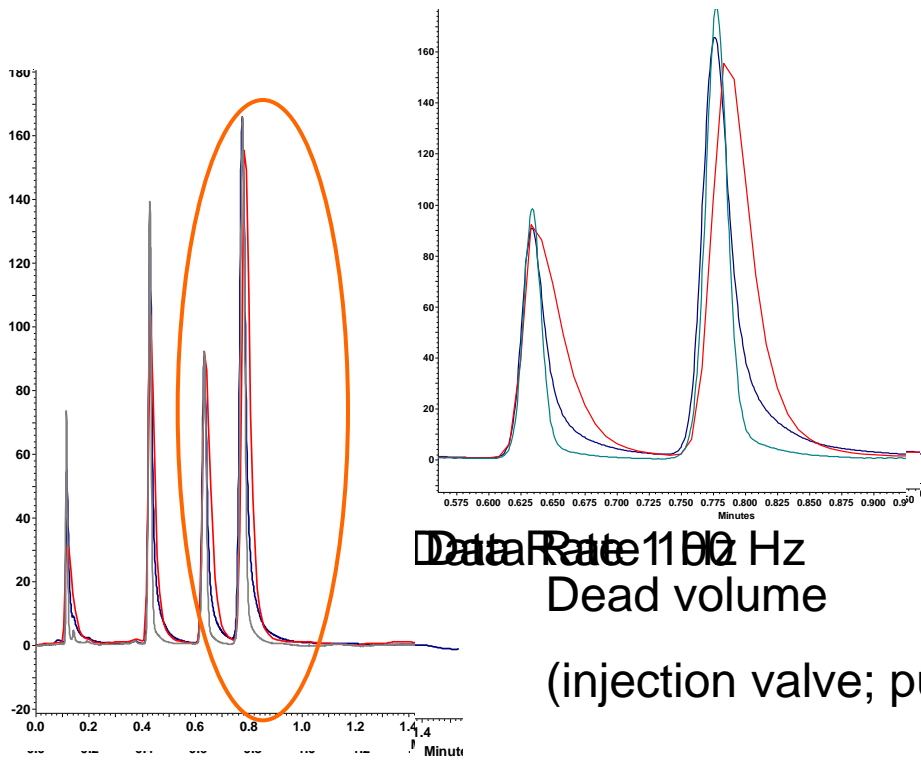


Permeability calculated without any corrections for temperature and pressure effects on viscosity (open squares). Permeability calculated with the effects of average temperature of the column on viscosity taken into account (closed triangles). Permeability calculated with both temperature and pressure effects on the viscosity taken into account (closed diamonds).



Separation of midazolam metabolites in rat bile.

- Why System Adaption ?



Data Rate 1100 Hz  
Dead volume

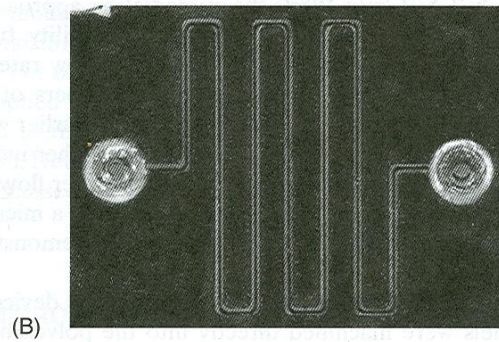
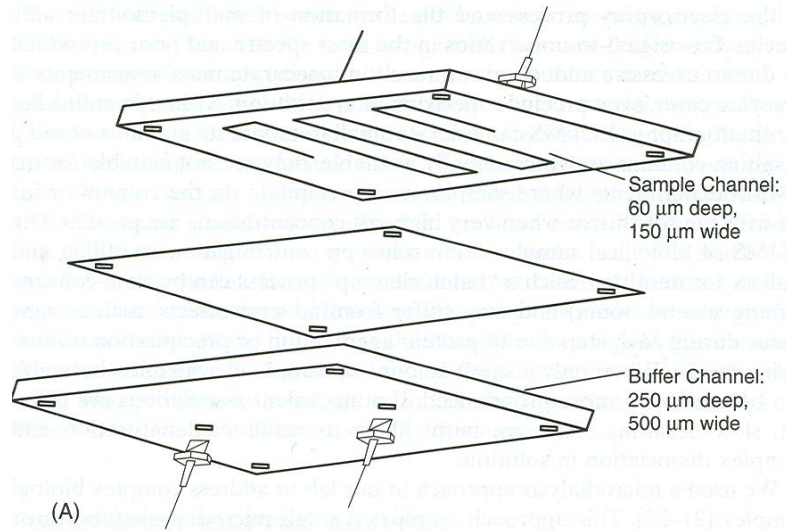
(injection valve; pump, UV cell, capillaries)



**Microchip**

# Introduction

- Microfabrication analytical devices are of growing interest because of their potential to enhance sensitivity and sample speed and to reduce instrument size, cost and weight.
- Most of the microanalytic devices reported have been fabricated on glass substrates using photolithography, wet chemistry and chemical etching processes. Recently, polymer materials have been used for preparation of chips. They have advantages such as; lightweight, chemically inert (glass chips require coating), easily fabricate and robust.



Microfluidation device

# Fabrication method

UV excimer laser were used to produce to produce microchannels of various geometries in polymeric materials.

Spot size: 10  $\mu\text{m}$

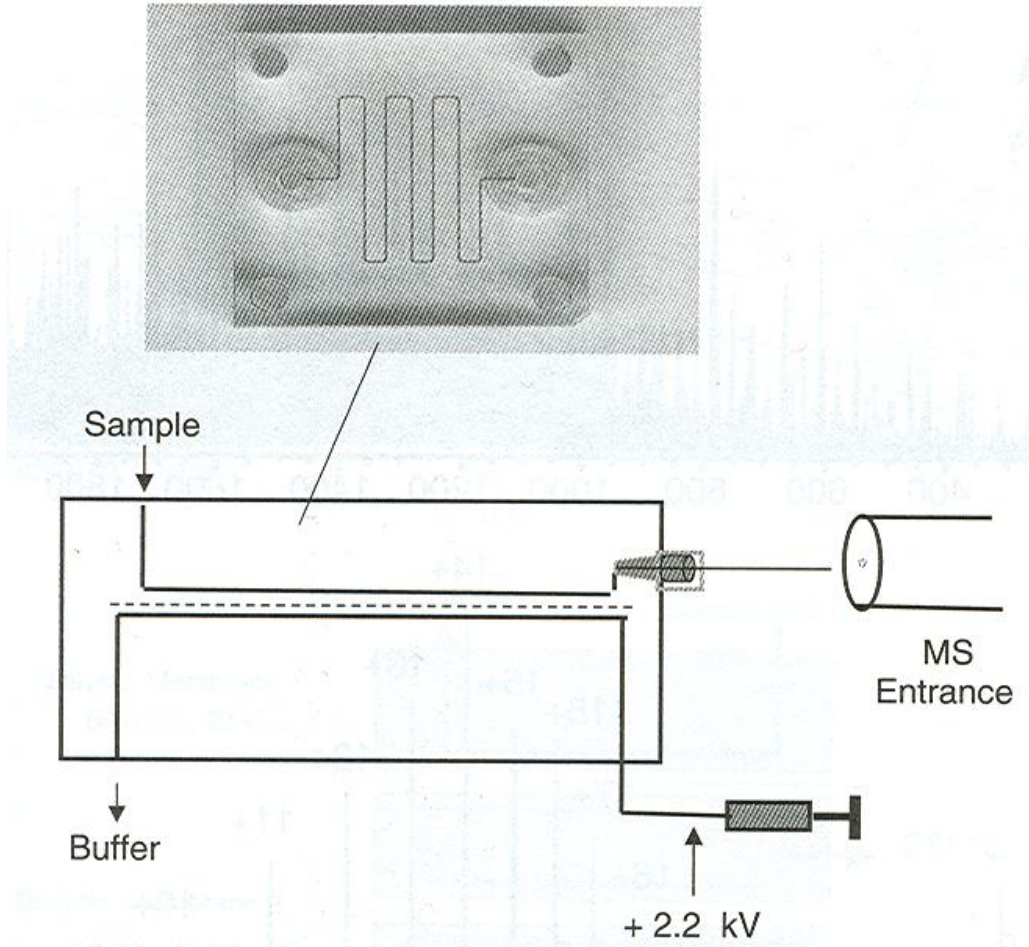
Repetition rate: 2 kHz

Pulse energy: 45  $\mu\text{j}$

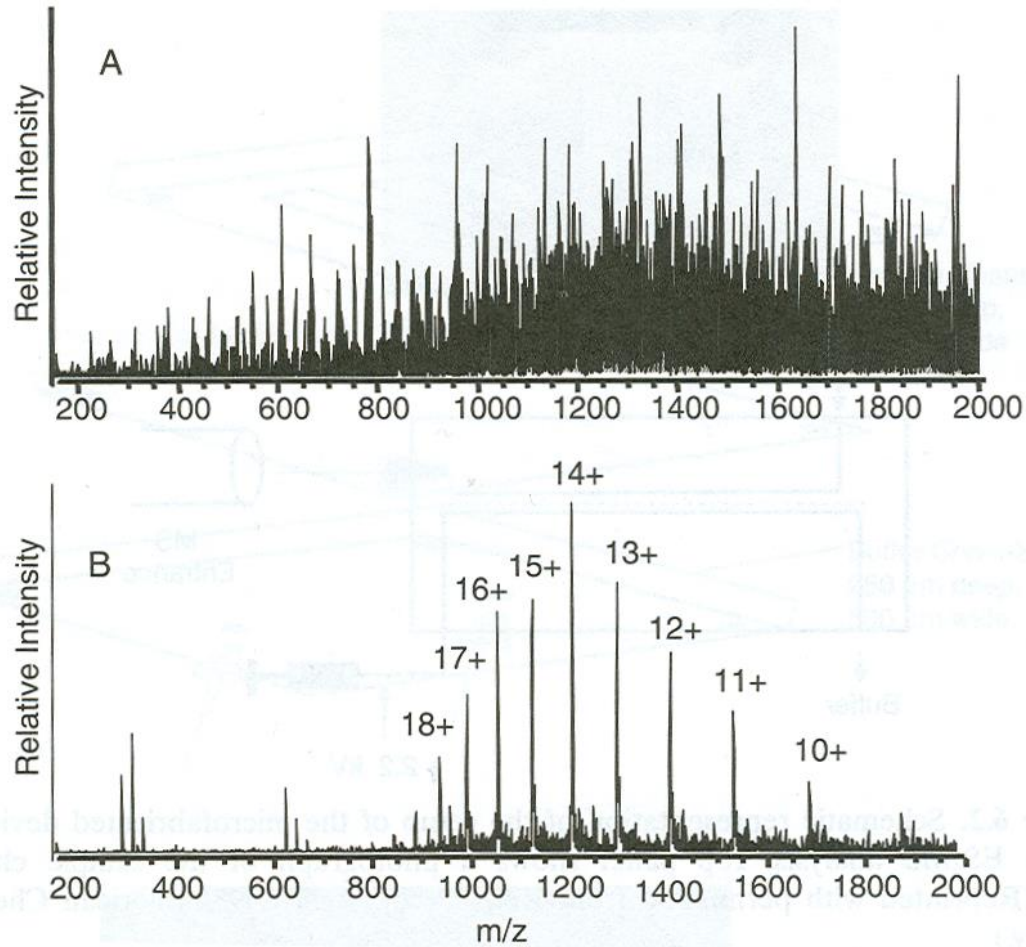


# Biological samples

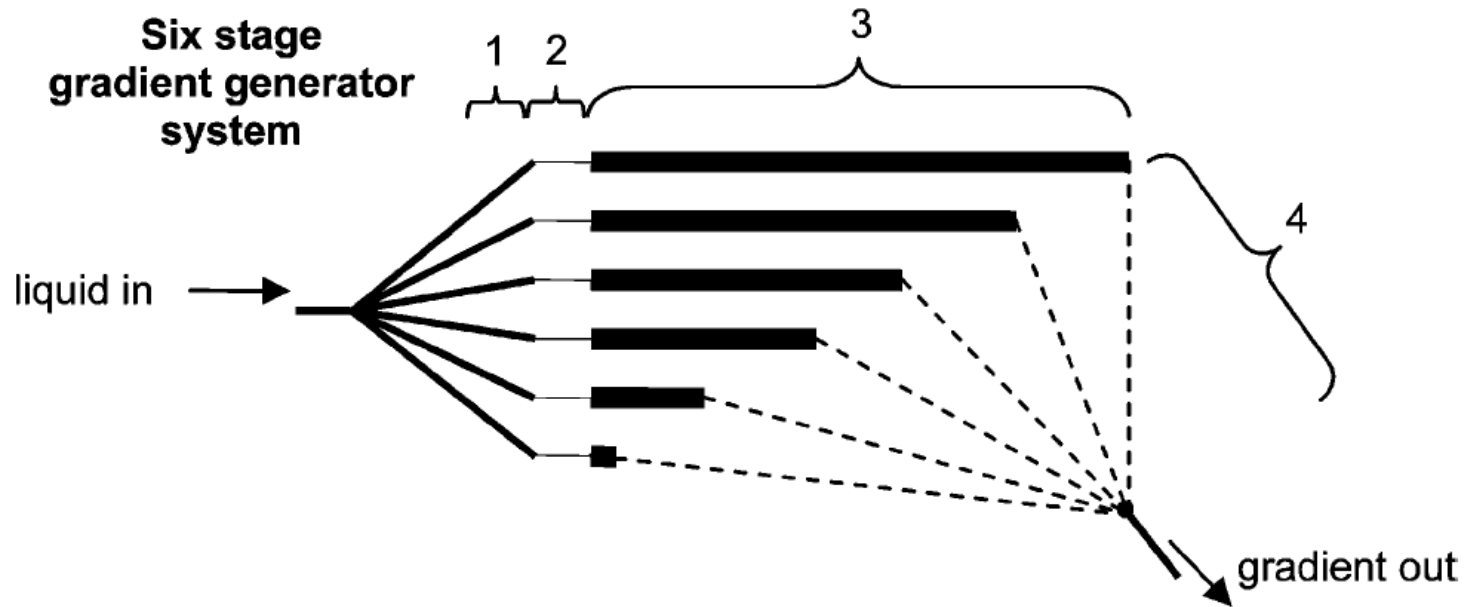
Biological samples extracted under physiological conditions (nonvolatile solvents, salts and other reagents) which not only affects on ESI but may also significantly reduce the analyte ion intensity and formation of multiple sodium adduct.



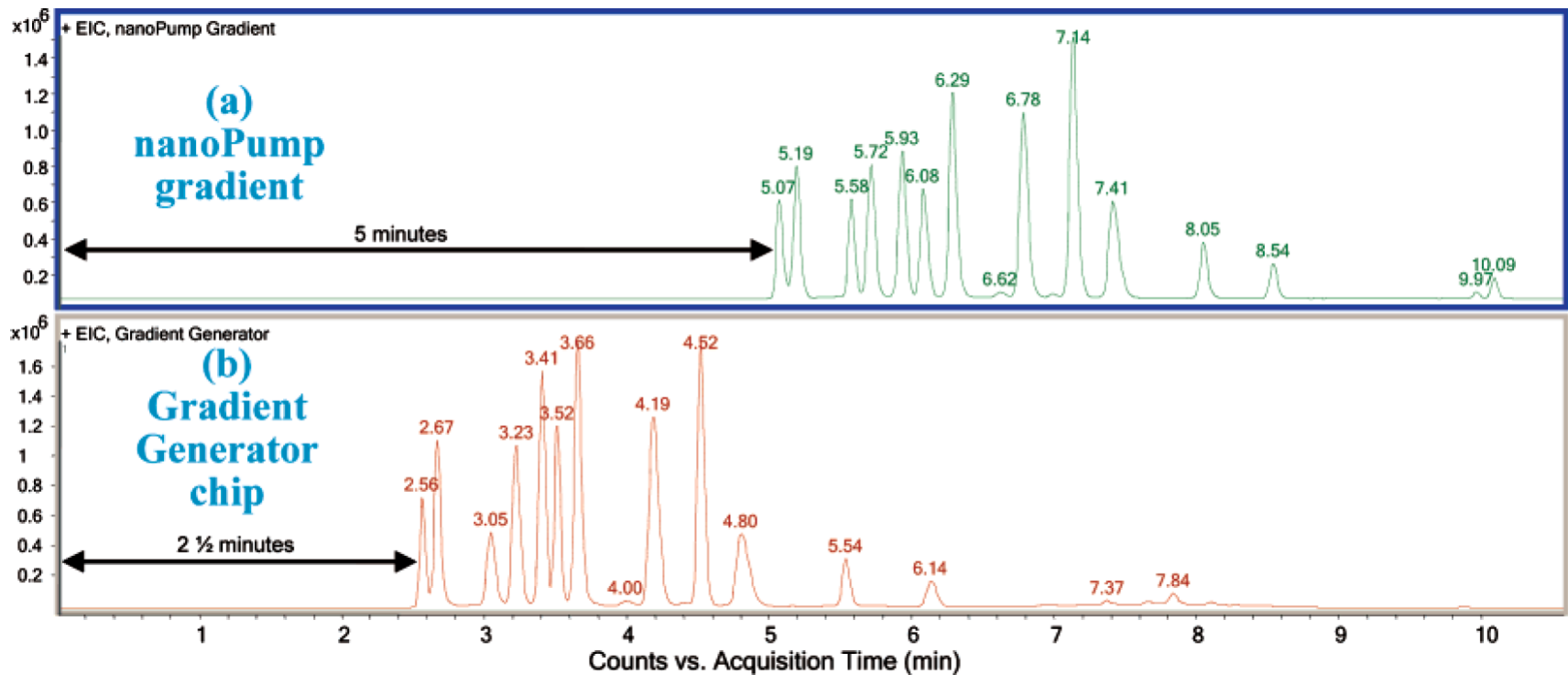
Microfractionation device for online ESI-MS



ESI-MS of 5  $\mu\text{M}$  horse heart myoglobin in biological fluid (a) without and (b) with dialysis chip.



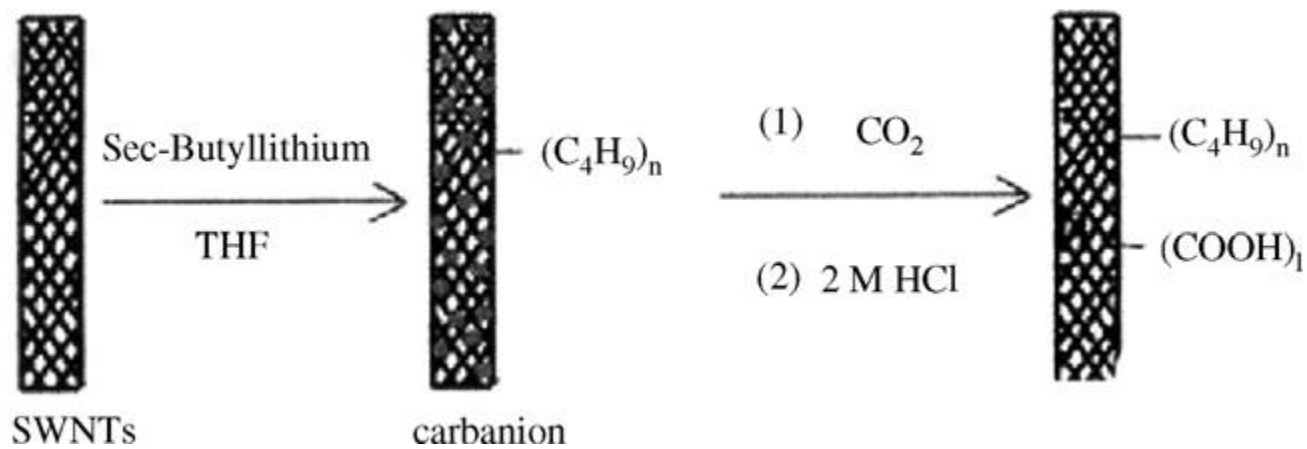
Schematic of a six-stage gradient generation concept. Each stage is made up of the four sections. Section 1 is the inlet manifold. Section 2 is the restrictor area. The section 3 timing channels define each stage's dwell time. Section 4 is the outlet manifold.



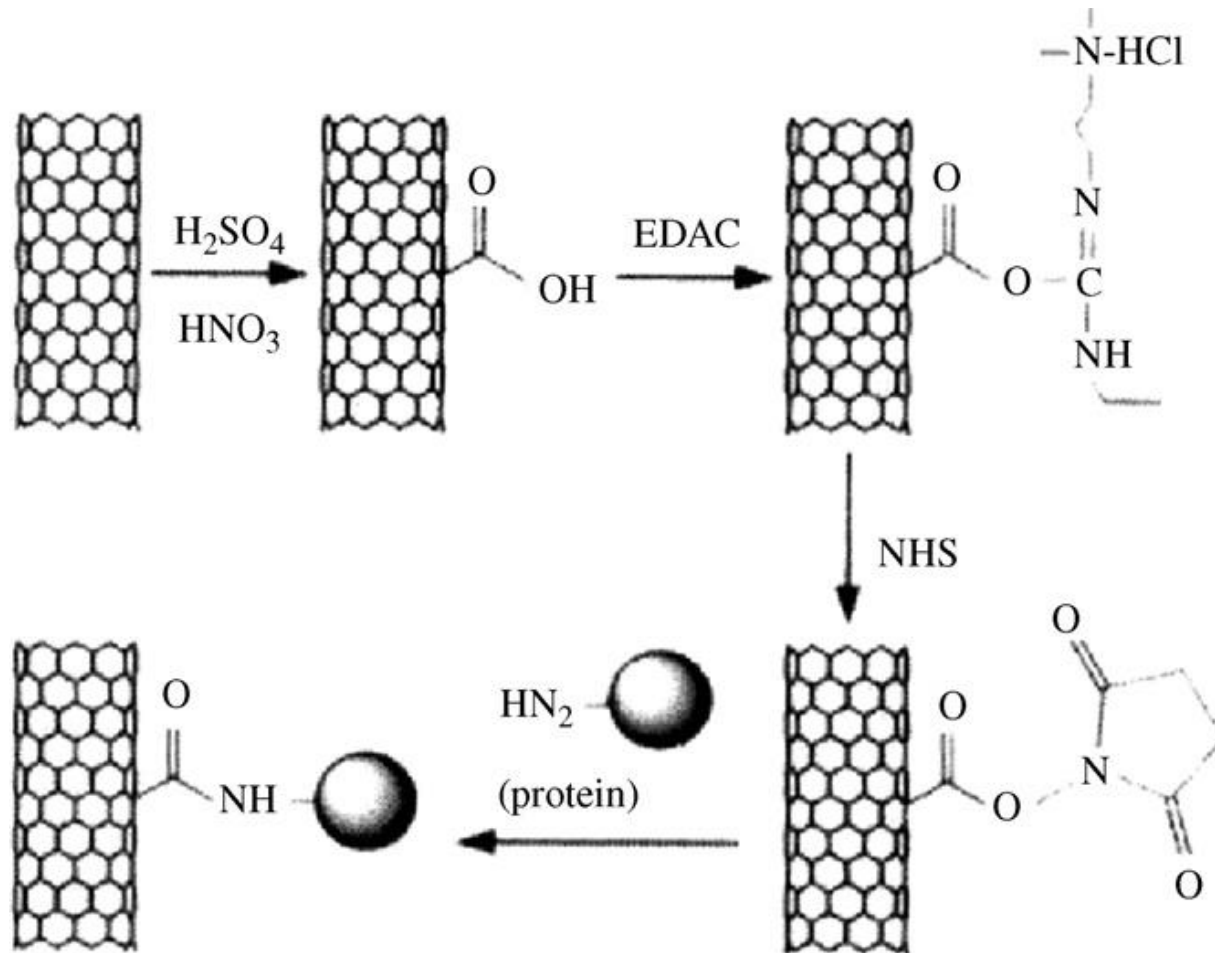
Experimental data comparing the separations and run times produced using (a) a standard nanoflow-pump-generated gradient and (b) a gradient generator chip gradient, both run at a 200 nL/min flow with the same HPLC-Chip. The sample is a 20 fmol/íL tryptic digest of BSA (1 íL injected). The plots are based on 12 extracted ions to increase the clarity of the plot, but the full data sets were similar as well.

# Nano Packing

## Schematic representation of the carboxylation of CNTs

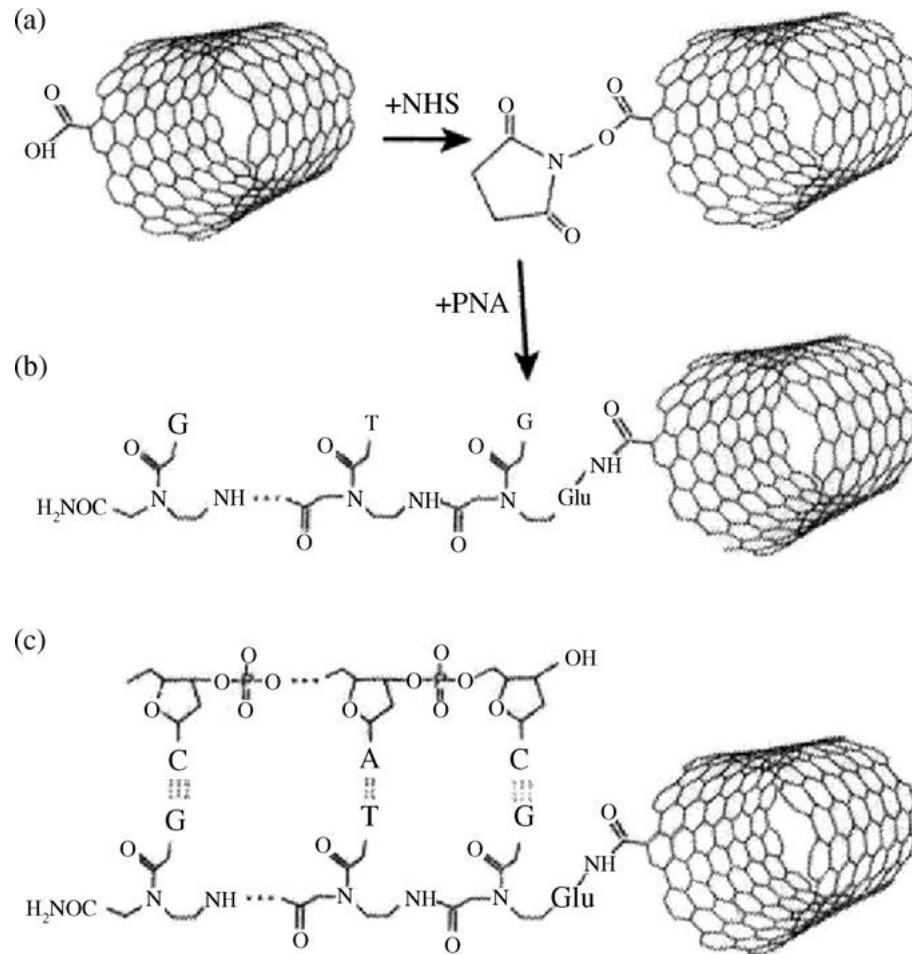


# Schematic view of the attachment of proteins to CNTs via diimide activated amidation





Attachment of DNA to CNTs. (a and b) *N*-Hydroxysuccinimide esters formed on carboxylated SWNT are displaced by peptide nucleic acid forming an amide linkage. (c) DNA fragment with a single-stranded sticky end hybridizes by Watson–Crick base-pairing to the PNA-SWNT

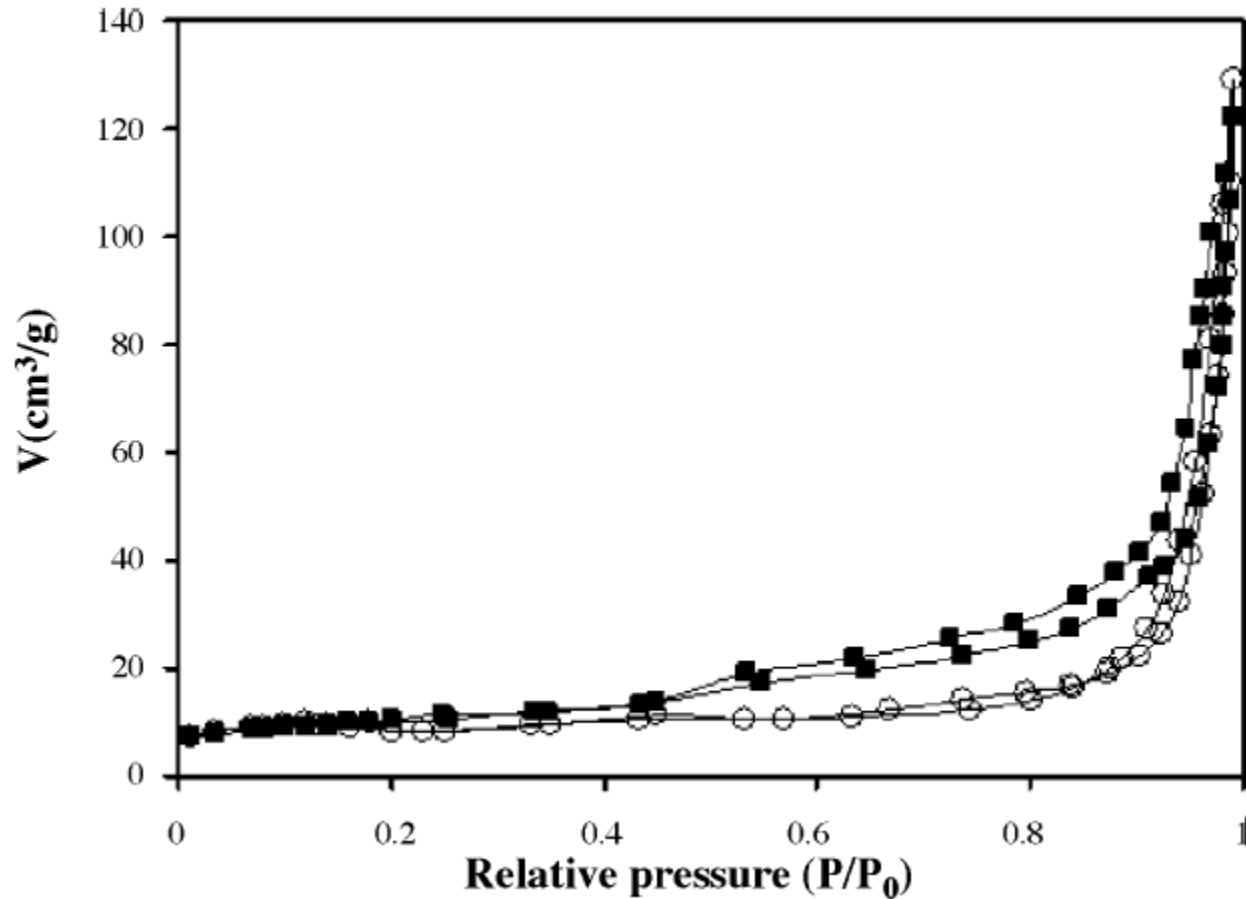


# Effect of carbon nanofiber functionalization on the adsorption properties of volatile organic compounds

- Montserrat R. Cuervo <sup>a</sup>, Esther Asedegbega-Nieto <sup>a</sup>, Eva D'iaz <sup>a</sup>, Aurelio Vega <sup>a</sup>, Salvador Ordóñez <sup>a,\*</sup>, *Eva Castillejos-López* <sup>b</sup>, *Inmaculada Rodríguez-Ramos* <sup>c</sup>
- *a Department of Chemical Engineering and Environmental Technology, University of Oviedo, Julián Clavería s/n, 33006 Oviedo, Spain*
- *b Departamento de Química Inorgánica y Técnica, Facultad de Ciencias, UNED, C/ Senda del rey, 9, 28040 Madrid, Spain*
- *c Instituto de Catálisis y Petroleoquímica, CSIC, C/Marie Curie nº 2, Campus de Cantoblanco, 28049 Madrid, Spain*
- *J. Chromatogr. A 1188 (2008) 264–273*

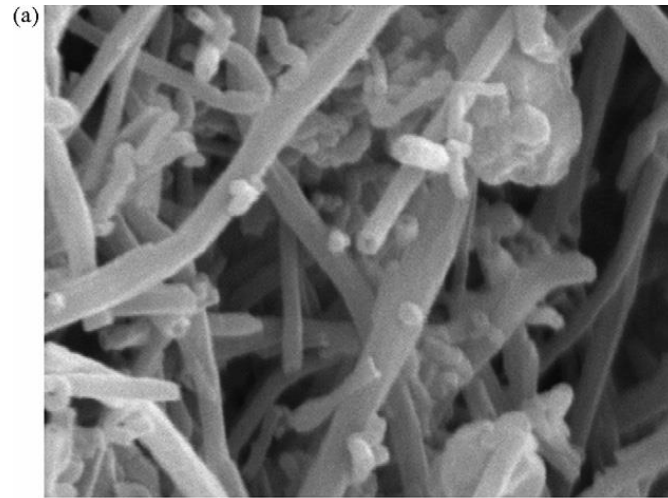
- CNFs are very hydrophobic materials almost without functional groups.
- The formation of oxygen-containing surface groups enhances the wettability properties of the CNFs, facilitating the preparation of well-dispersed catalysts and improving adsorption properties, especially for polar compounds.

Treatment in nitric acid increases the specific surface area, from the 32m<sup>2</sup>/g of the untreated sample to the 38m<sup>2</sup>/g of CNF-oxi,.

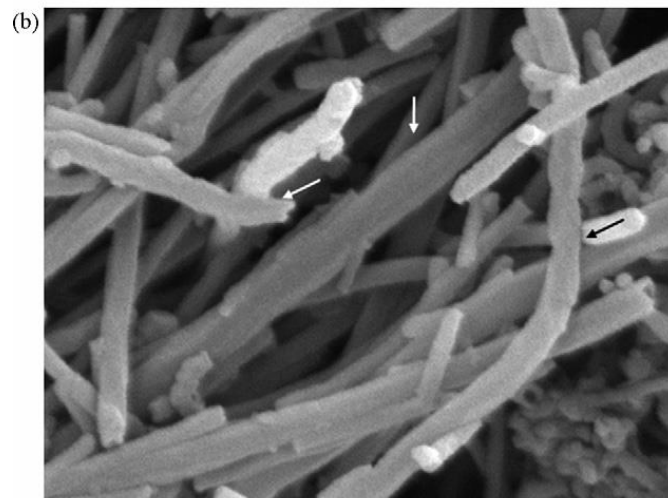


N<sub>2</sub> adsorption–desorption isotherms at –196 °C for CNF (○) and CNFoxi (■).

# SEM images of (a) CNF and (b) CNF oxidized with nitric acid.

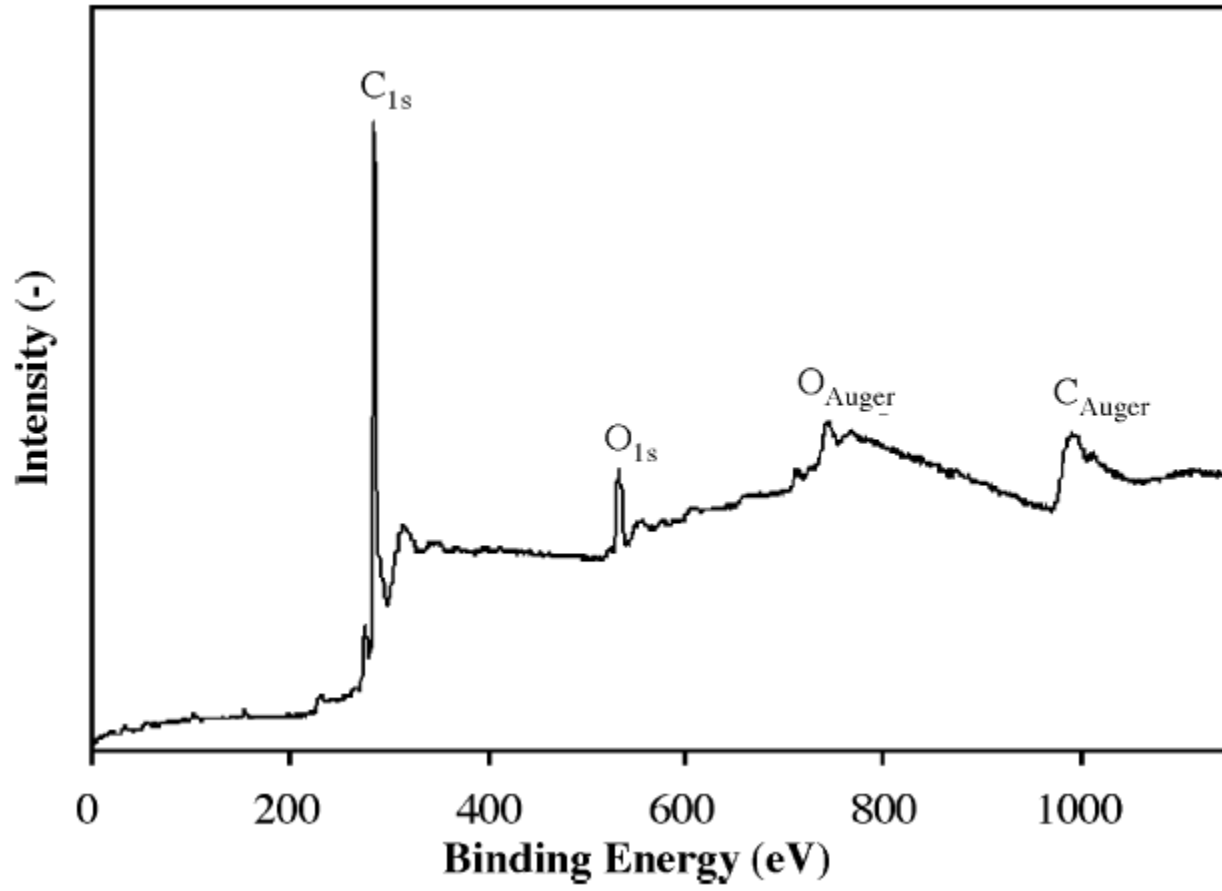


1 $\mu$ m

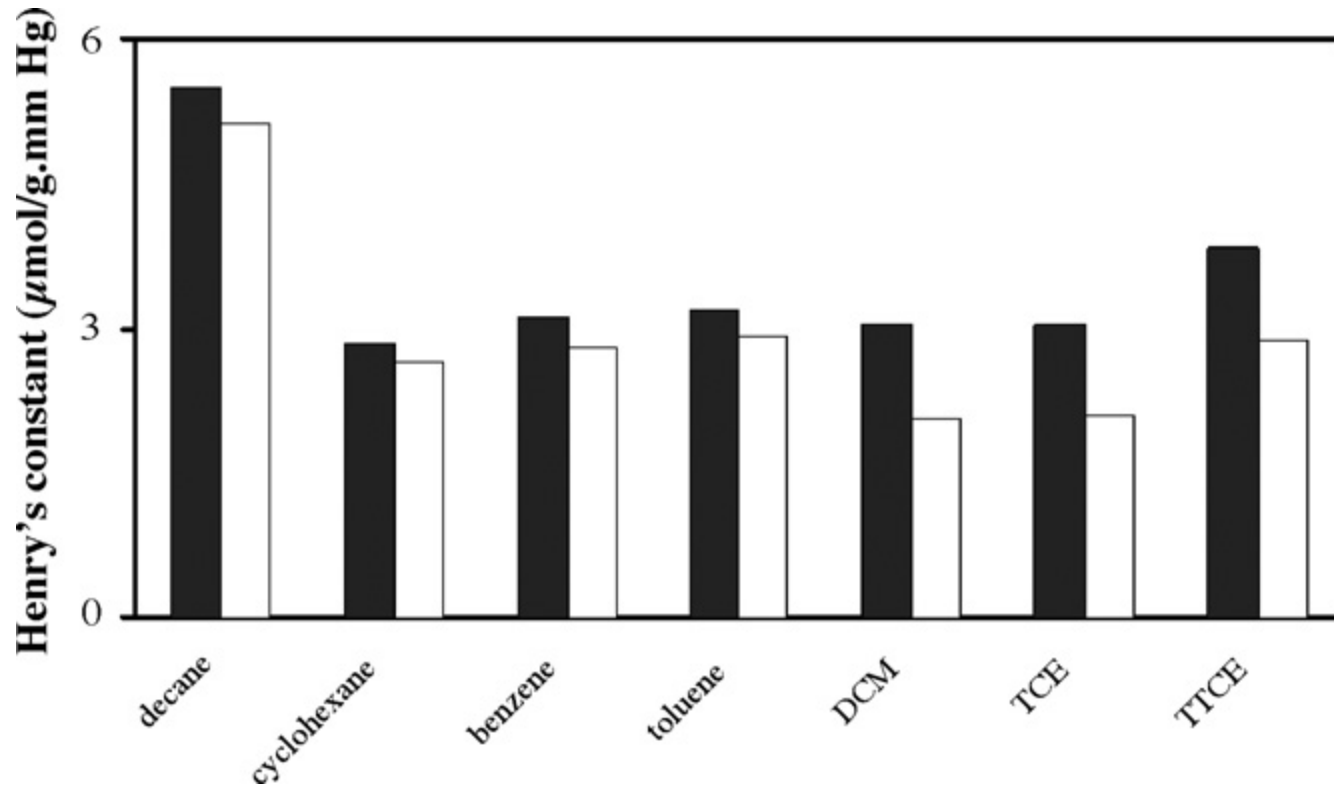


1 $\mu$ m

XPS survey spectrum, sample CNF-oxi.



Henry's constant for *n*-decane, cyclohexane, benzene, toluene, dichloromethane (DCM), trichloroethylene (TCE) and tetrachloroethylene (TTCE) over CNF (black) and CNF-oxi (white).

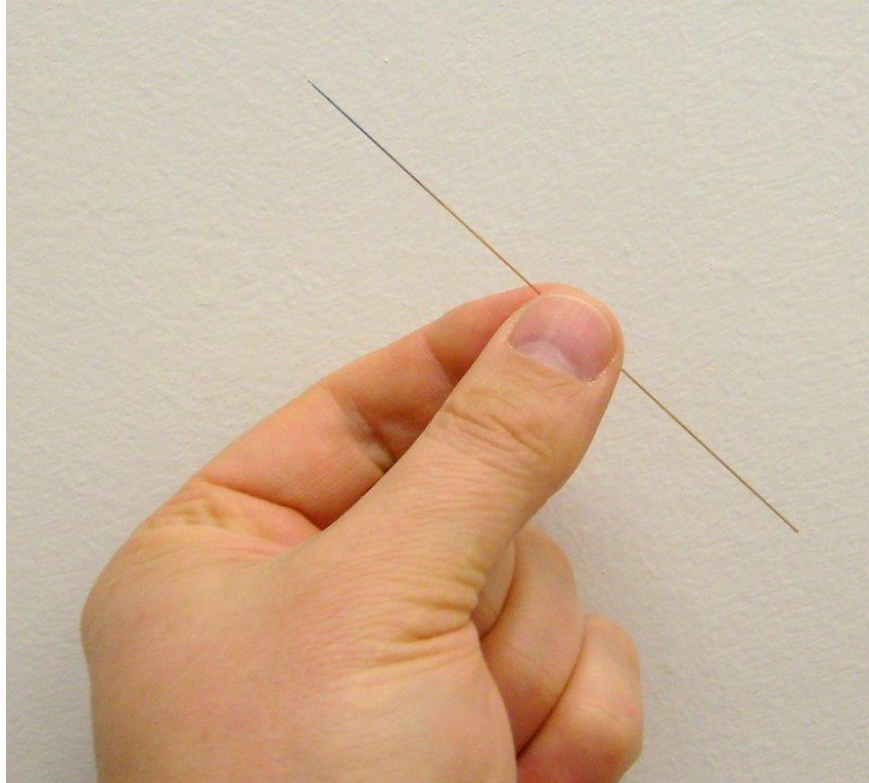


**Nano-LC**



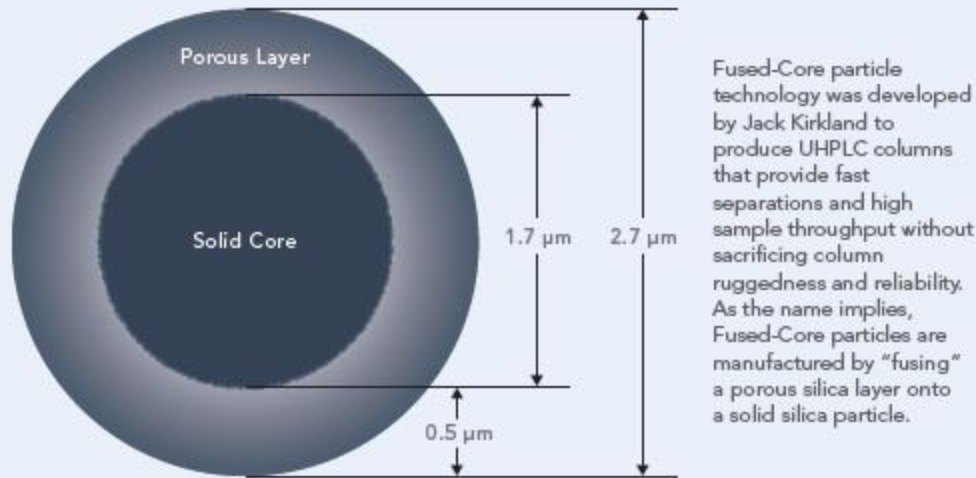
# Why miniaturization?

- i) increased mass sensitivity (in combination with concentration sensitive detection) owing to the reduced chromatographic dilution,
- ii) the use of smaller particle sizes ( $<2\ \mu\text{m}$ ) for the preparation of packed beds which—at a constant average flow velocity—translates into an increased efficiency because it reduces intraparticle stagnant mobile phase mass transfer resistance,
- iii) lower stationary phase, solvent, and sample volume consumption which facilitates the use of exotic liquids, expensive adsorbents, and/or long columns (if pressure drop is not a limiting factor), and
- iv) the compatibility with flow rate requirements of a nanoelectrospray interface for on-line coupling to mass spectrometry (MS).

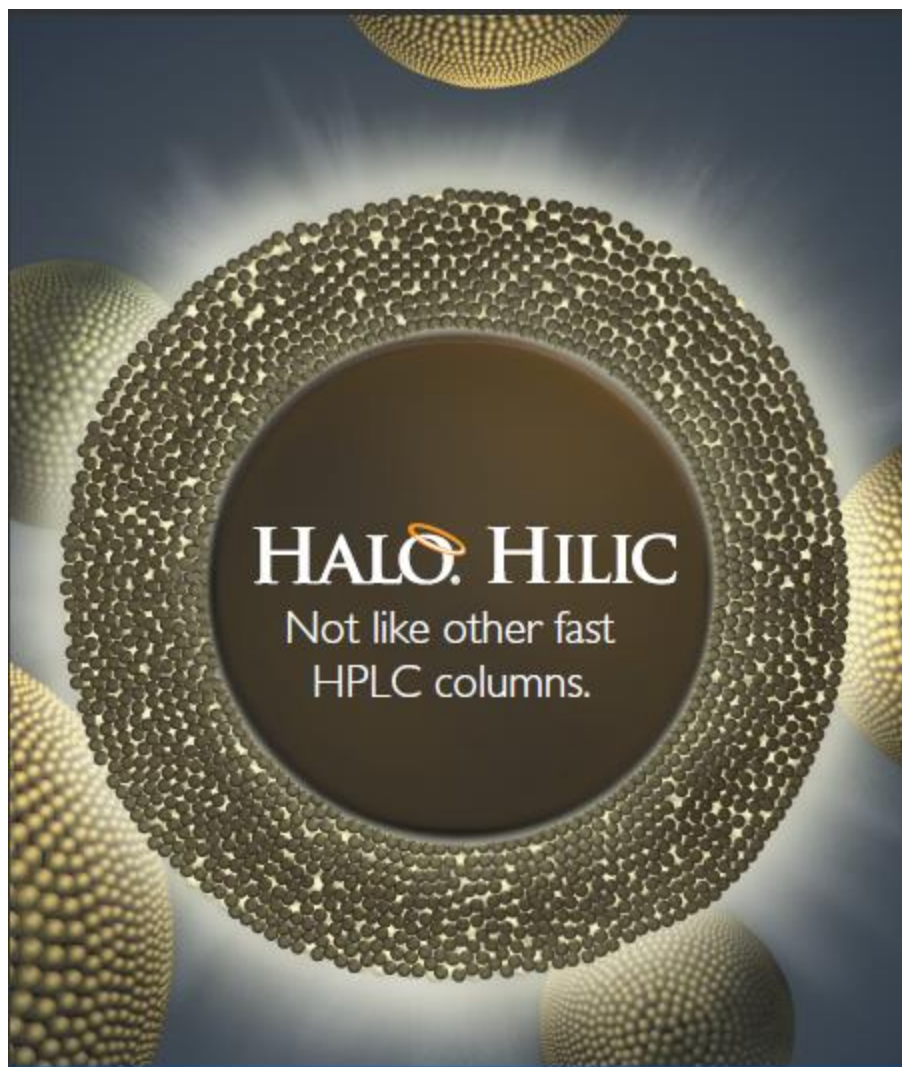


$$\Delta p = \frac{F \eta L}{\pi r^2 d_p^2}$$

**FIGURE 1:** HALO Fused-Core particle

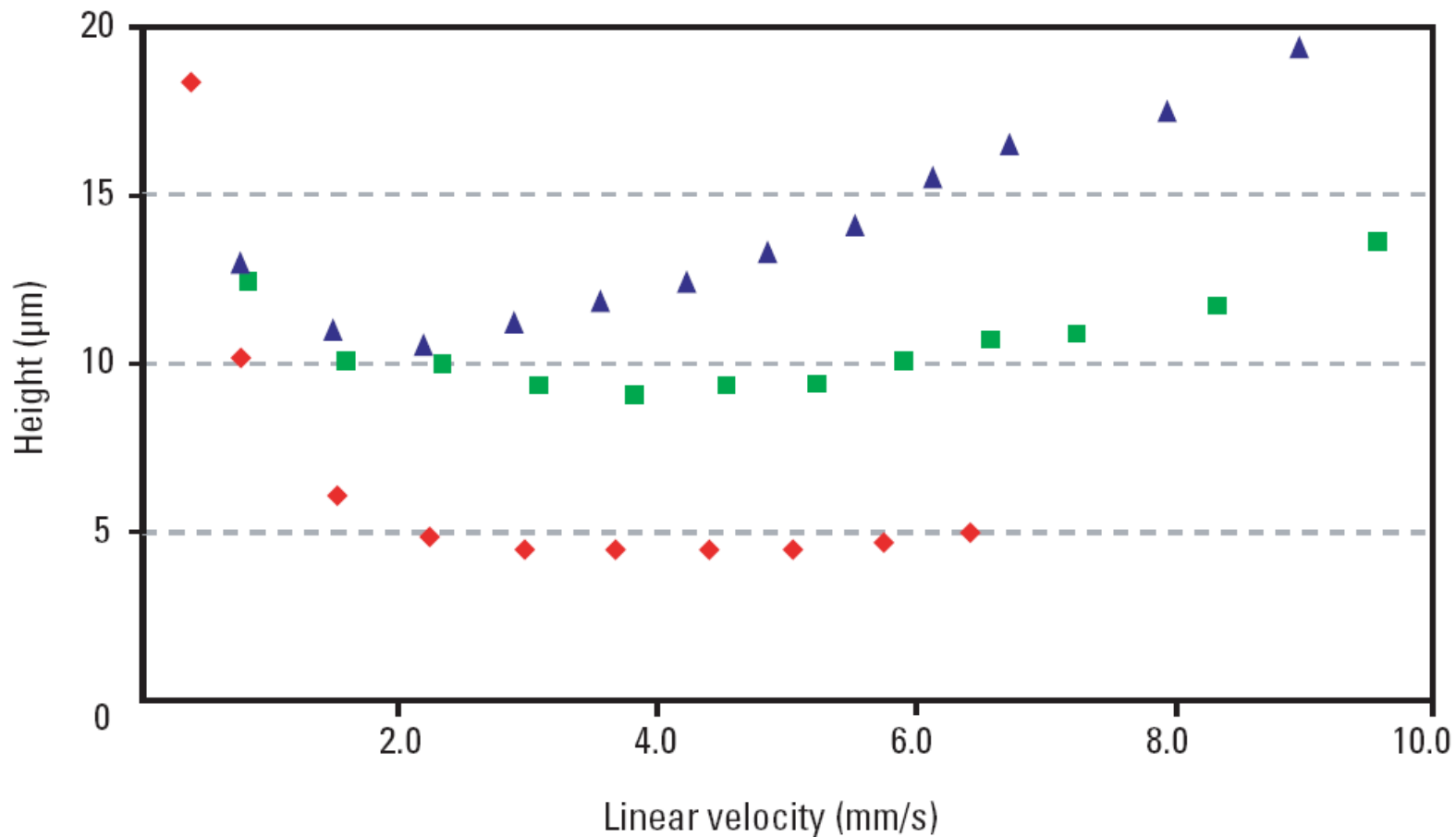


BACK PRESSURE - significantly less compared to UHPLC columns  
CONVENTIONAL HPLC EQUIPMENT can be used with near-UHPLC performance  
2 $\mu\text{m}$  INLET FRIT eliminates frit plugging problem  
FAST SEPARATION at high flow rates maintaining the resolving power



**HALO. HILIC**

Not like other fast  
HPLC columns.



Van Deemter curves for hexylbenzene on particles that are 1.7  $\mu\text{m}$  (red diamonds), 3.5  $\mu\text{m}$  (green squares), and 5.0  $\mu\text{m}$  (blue triangles) in diameter.

# Instrumentation of NanoLC

# Development of HPLC

Efforts to miniaturize HPLC in the 1980's led to the development of packed microcolumns using fused silica capillaries with a 20–250  $\mu\text{m}$  inner diameter and a flow rate of 0.02–10  $\mu\text{L}/\text{min}$  to gain higher sensitivity with higher separation efficiency.

In such microscale systems, absorbance-based detectors such as UV detectors are not suitable because shorter light paths lead to less sensitive detection.



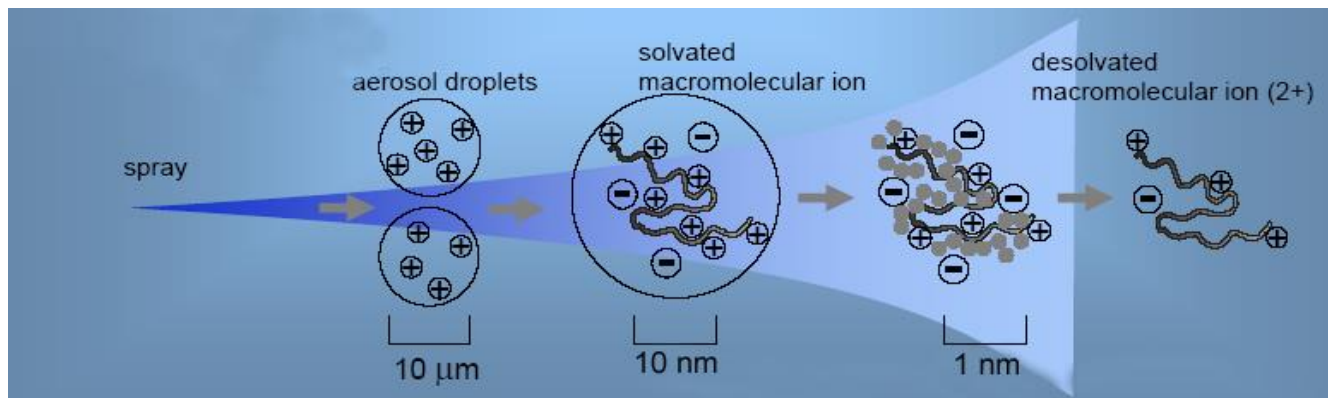
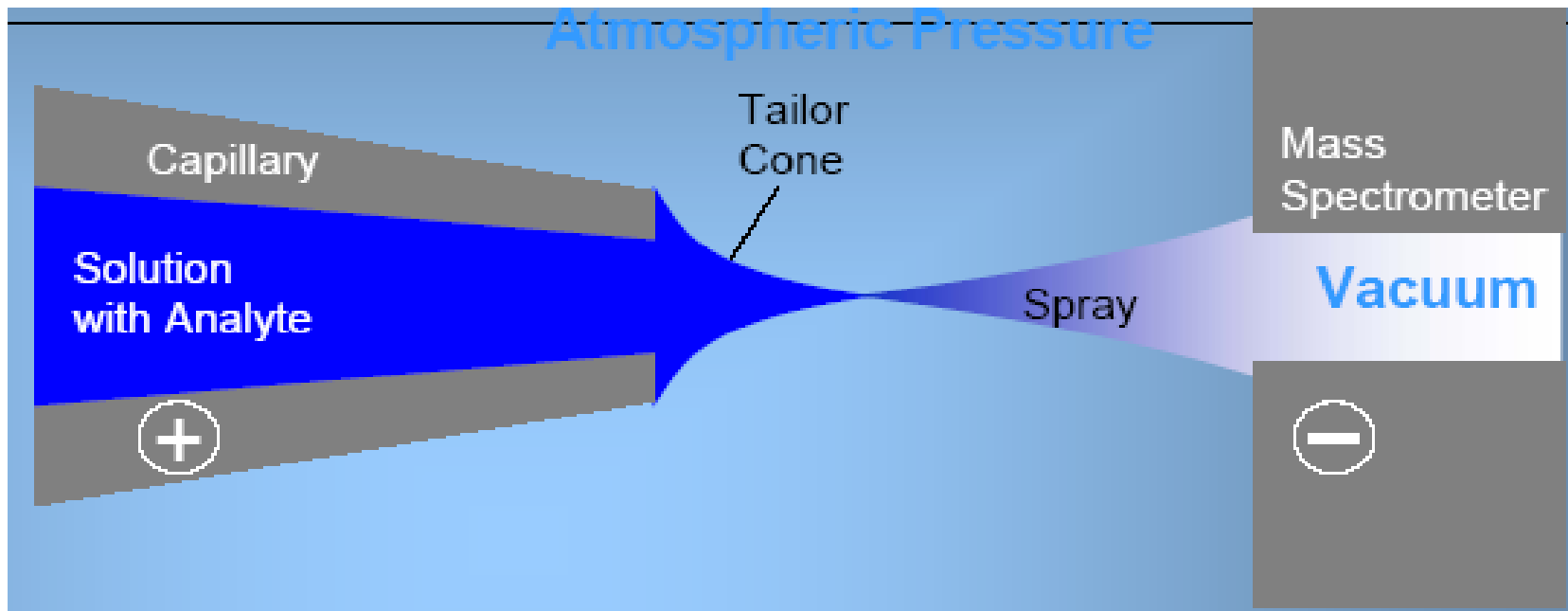
- Typical microcolumns for nanoLC are prepared using reversed phase materials with a 3–10  $\mu\text{m}$  diameter packed into fused silica capillaries with a 12–100  $\mu\text{m}$  diameter.

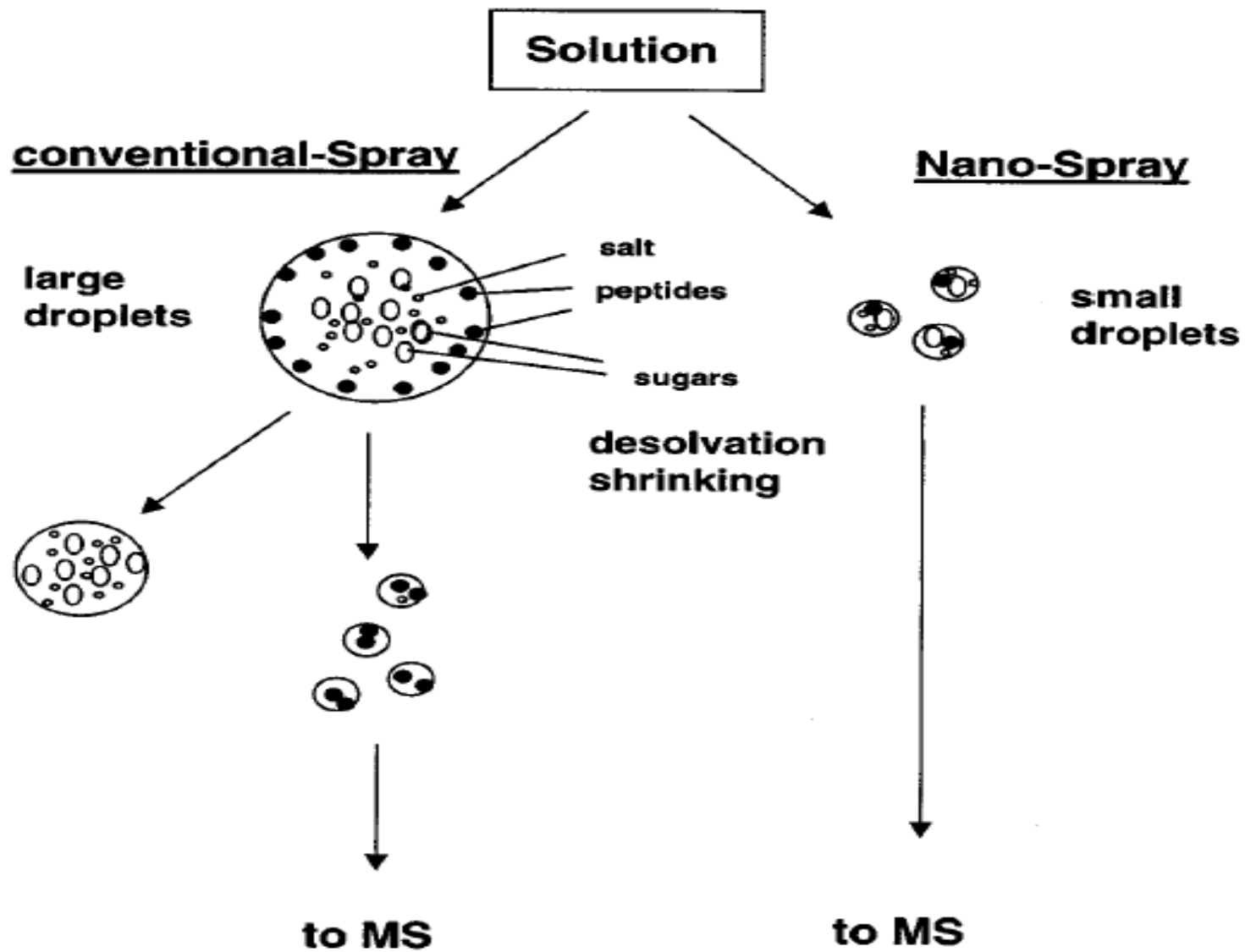
Flow range Category	Column ID (mm)	Flow rate Range ( $\mu\text{L}/\text{min}$ )	Optimum Flow ( $\mu\text{L}/\text{min}$ )	Analyte Capacity (g)
Analytical	4.6 or 4.0	750-1000	1000	$10^{-3}$ - $10^{-5}$
Narrowbore	2.0	100-1000	200	$10^{-5}$ - $10^{-9}$
Microbore	1.0	20-200	50	$10^{-6}$ - $10^{-19}$
Microbore	0.5	5.00-50.0	5.0	$10^{-7}$ - $10^{-11}$
Capillary	0.3	1.00-2.0	2.0	$10^{-8}$ - $10^{-12}$
Capillary	0.15-0.2	1.00-10.0	1.0-2.0	$10^{-9}$ - $10^{-3}$
Nano	0.075 or 0.1	0.10-1.00	0.15-0.5	$10^{-10}$ - $10^{-14}$
Nano	0.05	0.05-0.50	0.1	$<10^{-12}$

# Frit Problems

- In ESI-MS, a spray needle with a tapered outlet is used as a restrictor for packed particles to prepare a fritless column.
- A “stone-arch” column, where the opening size is two- to five-fold larger than the average particle size, and particles at the end of the column arch over the opening and these self-assembled particles function as a frit.
- Monolithic column do not require of frit (It should be considered that the lower loading capacity of monoliths is a potential problem in some cases).

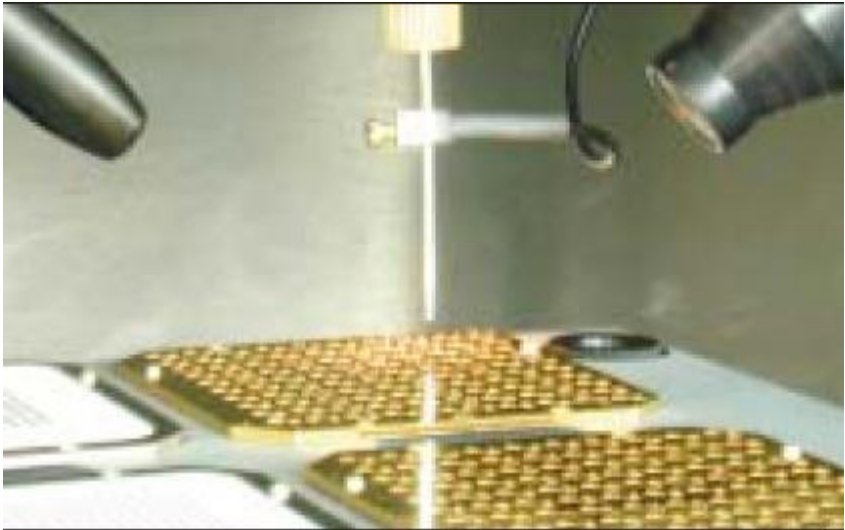
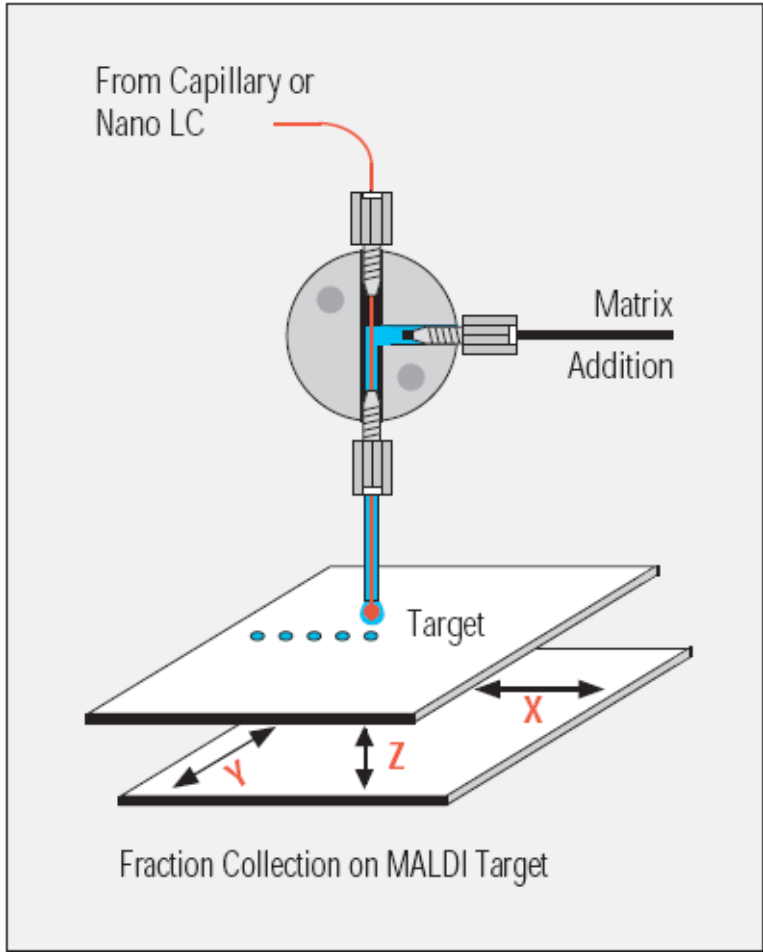
# LC ESI





# Nnao-LC MALDI

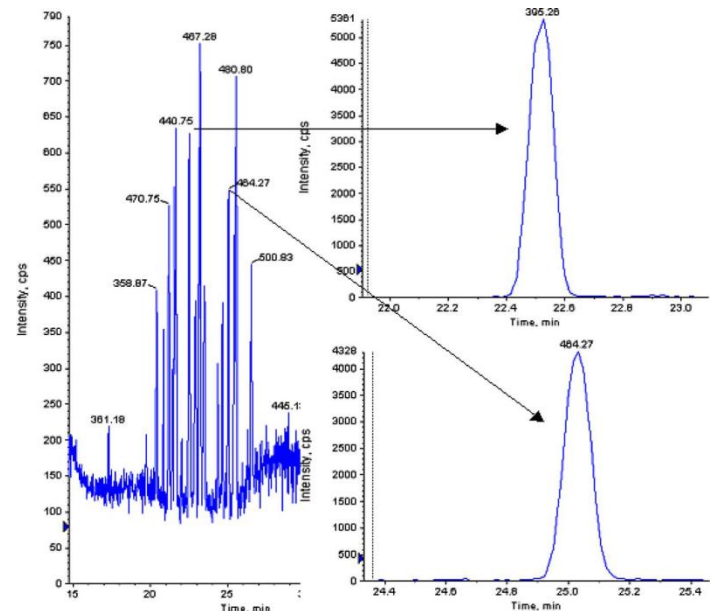
- There are two approaches of the liquid phase-MALDI interface. One is based on the on-line introduction of analytes into MS using a continuous flow. Another is based on the offline fractionation of analytes from LC eluent. In both modes, the MALDI matrix is mixed with analytes before introduction into the MS. In on-line aerosol liquid MALDI, an eluent mixed with the MALDI matrix is sprayed into a vacuum chamber of the MS to generate an aerosol, and the analyte is ionized from the aerosol by an irradiating laser. In off-line interfaces, analytes are directly deposited onto the target. For a target, a moving belt of cellulose membrane containing the matrix was reported first



# Mobile phase

- In LCMS for peptides, acidic conditions with ion-pair reagents are usually used in combination with C18 stationary phases to suppress peak broadening.
- Acetonitrile has been used as an organic solvent in many applications, but methanol gives better sensitivity in off-line infusion nanoES experiments; although in LC analysis the peak width is generally broader in methanolic buffers.

NanoLC–MS/MS analysis for 50 fmol tryptic digest of human serum albumin. Conditions: column, arch-stone C18 (100  $\mu\text{m}$  i.d., 150 mL, 6 m opening, ReproSil C18-3  $\mu\text{m}$ ); flowrate, 300 nL/min; mobile phase, 0.5% acetic acid with acetonitrile; gradient, acetonitrile 4–24% in 10 min; MS, AB-Sciex QSTAR pulsar i.

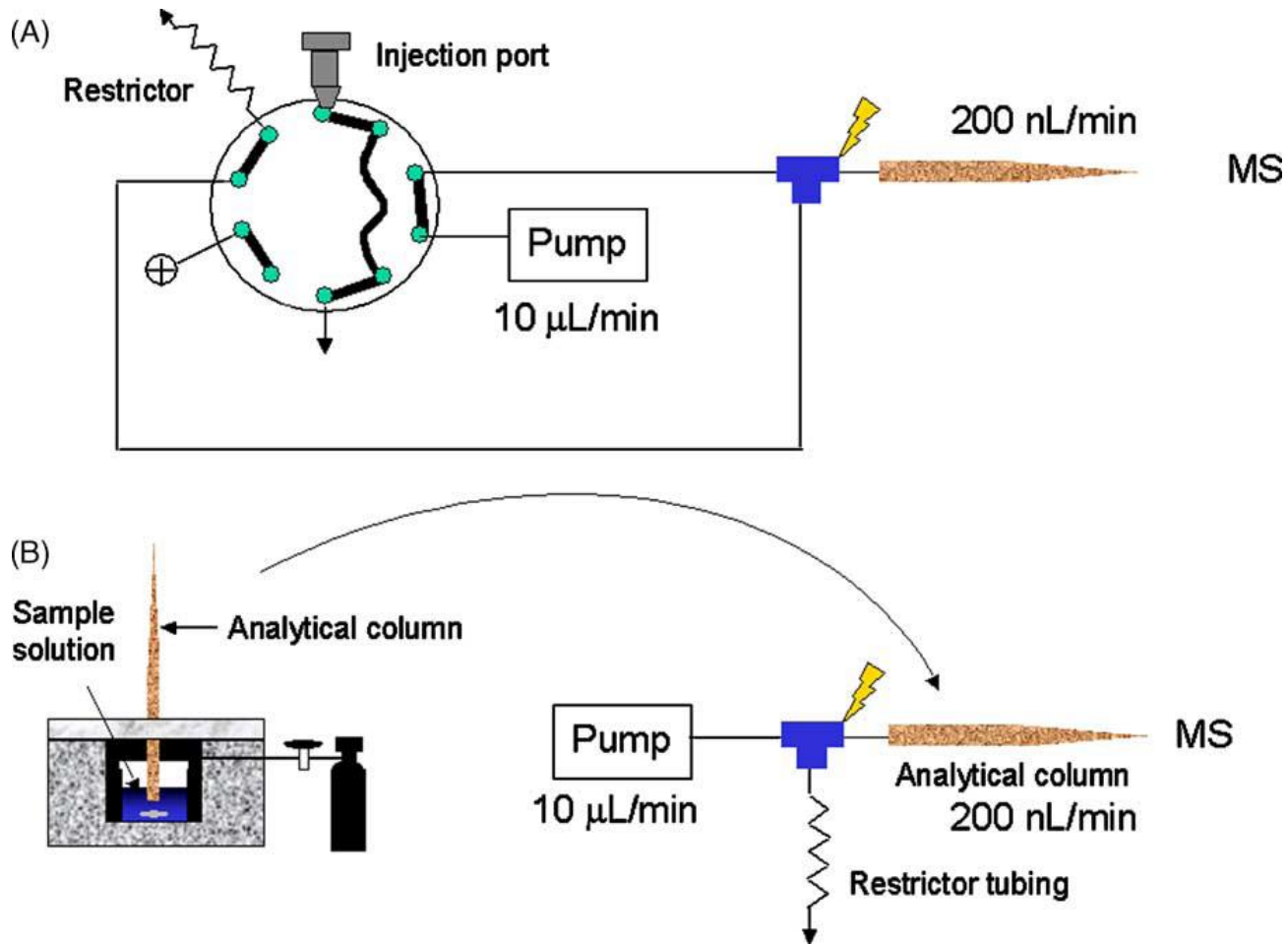


# *Injection system*

- Because of the low flowrate, injectors with a smaller dead volume such as injection valves with 100  $\mu\text{m}$  bore and 20–25  $\mu\text{m}$  i.d. transfer lines, should be used for nanoLC.



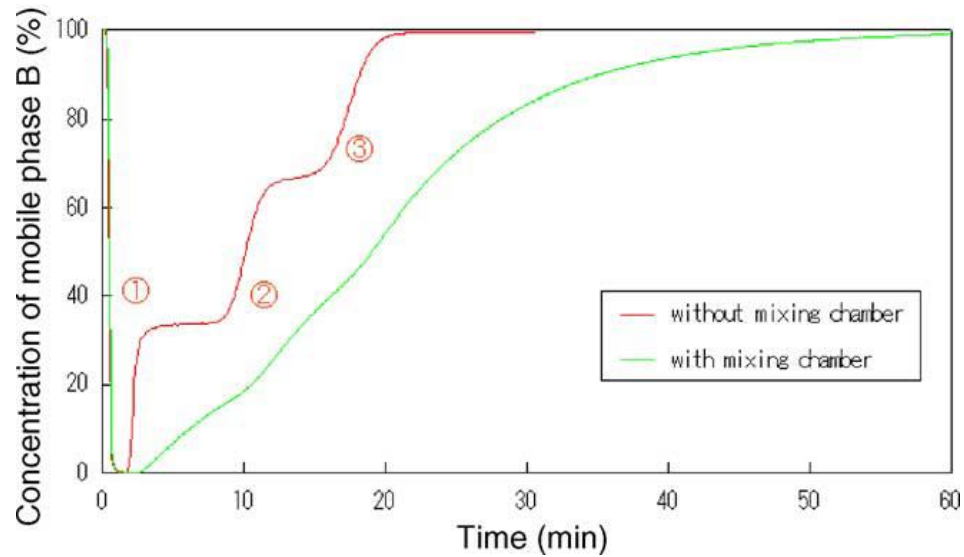
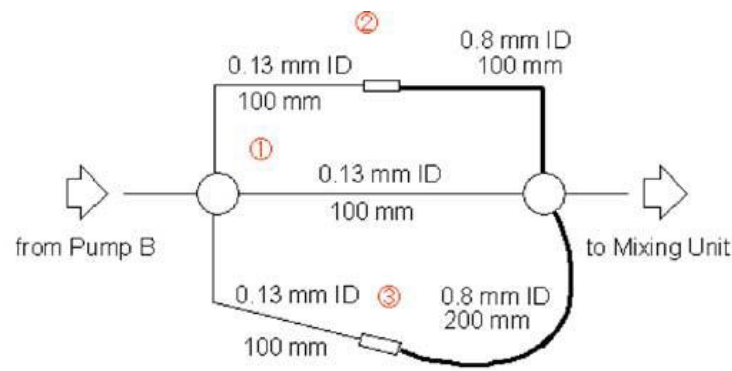
# Injection system



Direct injection systems without trap columns. (A) Using a 10-port injection valve. (B) Using an air-pressure cell.

# *Nano-flow gradient system*

- Two types of nanoflow pumps are currently available. One is a split type, where a splitter divides the higher flow rate generated by the pump into nanoflow.
- Another type of pump utilizes direct flow without flow splitting. Generation of a low flowrate less than 1  $\mu\text{L}/\text{min}$  in gradient mode is accomplished using a large mixing chamber in which the initial solvent is exponentially replaced with the final solvent.



Split tubing array (STAR) gradient systems. Top: STAR gradient generator using three split tubes with different restrictions and volumes. Bottom: Obtained gradient profiles with and without a mixing chamber.

# *Multidimensional separation*

- Although current nanoLC–MS/MS has a throughput of approximately 2000–4000 peptides per run within 1–2 h, it is not sufficient to analyze complex peptide mixtures such as that obtained from a whole cell lysate.
- On the other hand, the complexity problem can be solved by fractionation at both the protein and peptide levels. This leads to an increase in the total analysis time and the number of identified proteins becomes saturated as fraction number increases.
- Two factors, peak resolution and orthogonality to C18 separation, should be considered for peptide fractionation. For example, in SCX, to increase the resolution, linear gradient salt elution is preferable to step gradients, and the addition of organic solvents is effective to suppress hydrophobic interactions, i.e., to increase the orthogonality to C18 separation.

